



**HAL**  
open science

## **New development in carbon-based electrodes and electrolytes for enhancement of supercapacitor performance and safety**

Sirine Zallouz, Sergey Pronkin, Jean-Marc Le Meins, Cuong Pham-Huu,  
Camélia Matei Ghimbeu

### ► To cite this version:

Sirine Zallouz, Sergey Pronkin, Jean-Marc Le Meins, Cuong Pham-Huu, Camélia Matei Ghimbeu. New development in carbon-based electrodes and electrolytes for enhancement of supercapacitor performance and safety. *Renewable Energy Production and Distribution Volume 2 in Advances in Renewable Energy Technologies*, Elsevier, pp.353-408, 2023, 10.1016/B978-0-443-18439-0.00011-2 . hal-04299129

**HAL Id: hal-04299129**

**<https://hal.science/hal-04299129>**

Submitted on 22 Nov 2023

**HAL** is a multi-disciplinary open access archive for the deposit and dissemination of scientific research documents, whether they are published or not. The documents may come from teaching and research institutions in France or abroad, or from public or private research centers.

L'archive ouverte pluridisciplinaire **HAL**, est destinée au dépôt et à la diffusion de documents scientifiques de niveau recherche, publiés ou non, émanant des établissements d'enseignement et de recherche français ou étrangers, des laboratoires publics ou privés.

# New development in carbon-based electrodes and electrolytes for enhancement of supercapacitor performance and safety

Sirine Zallouz<sup>1,2</sup>, Sergey N. Pronkin<sup>4</sup>, Jean-Marc Le Meins<sup>1,2,3</sup>, Cuong Pham-Huu<sup>4</sup>, Camélia Matei Ghimbeu<sup>1,2,3</sup>,

<sup>1</sup> Université de Haute-Alsace, Institut de Science des Matériaux de Mulhouse (IS2M), CNRS UMR 7361, F-68100 Mulhouse, France

<sup>2</sup> Université de Strasbourg, F-67081 Strasbourg, France

<sup>3</sup> Réseau sur le Stockage Electrochimique de l'Energie (RS2E), FR CNRS 3459, 80039 Amiens Cedex, France

<sup>4</sup> Institut de Chimie et Procédés pour l'Energie, l'Environnement et la Santé, ICPEES, CNRS UMR-7515, 67087 Strasbourg, France

## **Abstract**

This book chapter presents an overview on the electrode materials and electrolytes used in supercapacitors. The working principles, the mechanisms of charge storage, and the configuration of supercapacitors are briefly discussed. A first focus is on electrode materials relying on different charge storage mechanisms, i.e., electrochemical double-layer carbon materials and pseudocapacitive transition-metal oxides and metal-sulfides materials. The last part focuses on the electrolytes used in supercapacitors. Classical liquid electrolytes are reviewed and the development of gel- and solid-like electrolytes is presented. The advantages, current limitations, and challenges of electrodes and electrolytes are also addressed.

**Keywords:** supercapacitor; carbon; metal oxide; metal sulphide; electrolyte;

## Table of contents

I.	General introduction .....	3
II.	Supercapacitors: Stat-of-the-art .....	4
II.1.	Brief history and definition of a supercapacitor .....	4
II.2.	Mechanisms of energy storage .....	6
II.2.1.	Electrochemical double layer capacitors (EDLC) .....	6
II.3.	Types of supercapacitors .....	11
II.3.1.	Symmetric supercapacitors .....	11
II.3.2.	Asymmetric supercapacitor .....	14
III.	Electrode materials .....	19
III.1.	Carbon Materials .....	19
III.1.1.	0D carbon materials .....	20
III.1.2.	1D Carbon .....	21
III.1.3.	2D Carbon .....	21
III.1.4.	3D Carbon .....	24
III.2.	Carbon/ transition metal oxide composites .....	25
III.3.	Carbon/ metal sulfide composites .....	28
IV.	Electrolytes .....	30
IV.1.	Liquid electrolytes .....	31
IV.1.1.	Aqueous electrolytes .....	31
IV.1.2.	Organic electrolytes .....	32
IV.1.3.	Ionic Liquids .....	32
IV.2.	Solid-like electrolytes .....	33
IV.2.1.	Gel electrolytes .....	33
IV.2.2.	Solid electrolytes .....	35
V.	Conclusion .....	39
	References .....	41

## I. General introduction

The population of Earth is constantly increasing and accordingly our needs in transportation, resources and energy. This leads to a sharp increase in the consumption of fossil fuels. As a consequence, the environmental problems such as climate change related to greenhouse gas emissions are increasing along with the water and the air pollution. Moreover, fossil fuel reserves are limited and are unevenly distributed on our planet creating geo-political tensions. Tackling these issues requires the development of new energy sources, but also technologies for efficient energy transportation and storage. Thus, there is an urgent need to progress on the conception of energy storage devices that provides the energy when needed.

The importance of electrochemical energy storage devices (EESD) is attested by the 2019 Nobel Prize awarded for the discovery and development of lithium ion batteries.<sup>1</sup> Among the EESD, the most commonly used are batteries and supercapacitors, which have complementary characteristics. Batteries are used whenever high energy density is needed, whereas supercapacitors are more adapted for applications requiring high power density, namely when energy uptake occurs in short time period, such as automotive kinetic energy recovery system (KERS) and opening emergency doors of airplanes.<sup>2</sup> Supercapacitors are also increasingly demanded due to rapid development of flexible and wearable electronics. The attention is directed towards ecological, high-performing, and long-life devices. The research challenges are focused on practical requirements such as light and ultrathin devices,<sup>3</sup> but also on expanding the life of EESD. For this purpose, novel electrode materials and a new type of electrolytes are being developed.

Today, commercial supercapacitors use mostly carbon with high surface area as electrode material and generally organic liquid electrolytes. However, other types of electrode materials are promising for supercapacitors, such as transition metal oxides (TMO) and transition metal sulfides (TMS). All of these categories of electrode materials will be discussed in detail in the first part of this chapter. The mechanisms of charge storage by formation of an electrical double layer and pseudocapacitance are briefly summarized for better understanding. Lastly, the latter section is dedicated to the description of electrolytes used in supercapacitors. A classification of conventional liquid electrolytes will be provided, as well as their interaction with electrode materials. Moreover, the emerging development of gel and solid-like electrolytes is presented. A comparison between the two families is proposed and their advantages, current limitations and challenges addressed.

## II. Supercapacitors: Stat-of-the-art

### II.1. Brief history and definition of a supercapacitor

The electrostatic capacitor concept was demonstrated firstly in 1745 by Leyden Jar, using a glass container acting as a dielectric separator and metal external and internal foils as electrodes.<sup>4</sup> The capacitance of a simple capacitor is given by Eq. 1.

$$C = \frac{\epsilon_0 \epsilon_r A}{d} Eq. (1)$$

Where:  $C$  is the capacitance in F,  $\epsilon_0 = 8.85 \cdot 10^{-12} F m^{-1}$  is the electrical permittivity of vacuum,  $\epsilon_r$  is the dielectric constant of a separator,  $A$  is the electrochemically accessible surface area ( $m^2$ ) and  $d$  is the distance between the electrodes (m). Therefore, surface specific capacitance  $C_s = C/A$  is dependent on the distance  $d$  and dielectric constant of separator  $\epsilon_r$ .

In the 19<sup>th</sup> century, the electric double layer (EDL) model of electrode/electrolyte interface was proposed by the German physicist Helmholtz. He suggested a compensation of a free charge of the electrode by electrostatic adsorption of the opposite electrolyte charged ions at a distance  $d$ , forming an interfacial capacitor with capacitance given by Eq.1. Afterwards, Gouy, Chapman and Stern improved this model.<sup>5</sup>, as will be further discussed in more detail.

Contrary to electrostatic capacitors, the parameters (namely  $d$  and  $\epsilon$ ) determining surface specific capacitance of electrochemical interface,  $C_s$  in pseudocapacitors, are potential-dependent. Depending on the mechanism of charge storage (see II.2), the potential dependence of charge storage capacitance can be negligible, as in pure EDL materials, significant, as in some pseudocapacitive materials, and very significant in batteries-like materials.

In general, the terms supercapacitors, electrochemical capacitors (ES) or ultracapacitors are used to describe the same device. They could be defined as a class of EESD that has charging behavior similar to that of electrostatic capacitors (contrary to batteries), namely weak dependence of charge capacitance and energy density on applied voltage and charging rate.

The performance of electrode materials is conventionally compared in terms of mass-specific capacitances ( $C_m$ ) or volume-specific capacitances (CV).

$$C_m = C_s \cdot SSA$$

$$C_V = C_s \cdot SSA \cdot \rho$$

Here, SSA is specific surface area, that is, surface area of 1 g of a material, and  $\rho$  is the density of the material.

Energy storage devices are characterized by energy capacitance  $E$  and power  $P$ . For supercapacitors, the energy and power are calculated according to Equations 2 and 3:

$$E = \frac{1}{2} C_m V^2 E q. (2)$$

$$P = \frac{V^2}{4 \cdot R \cdot m} = \frac{E}{t} E q. (3)$$

Where:  $C_m$  is mass-specific device capacitance,  $V$  is the voltage of the device,  $E$  is the energy density  $R$  is the system resistance  $t$  is the discharge time and  $P$  is the power density.

The energy storage in supercapacitors is faster than in batteries and makes the former ones capable of maintaining high power rates (above 10 kW kg<sup>-1</sup>). The so-called Ragone plot is used to classify the different energy storage technologies as presented in Figure 1. One can see that supercapacitors are particularly interesting as they fill the gap between simple capacitors and batteries. On the one hand, their specific energy is several orders of magnitude higher than that of capacitors, and on the other hand, their specific power is significantly higher than that of batteries.

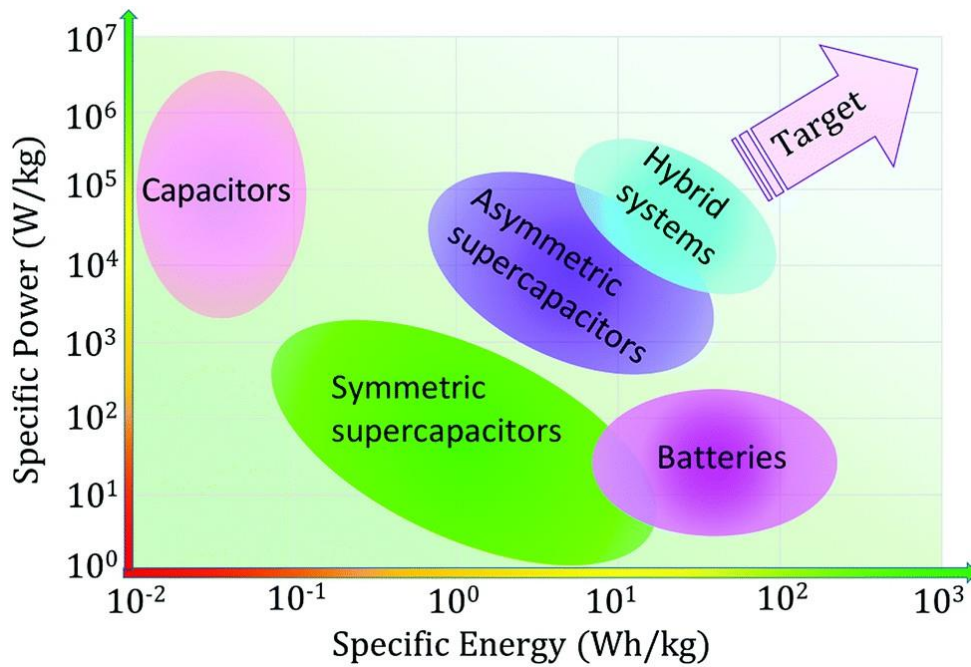


Figure 1 Ragone plot for different energy storage devices. Used with permission of Royal Society of Chemistry, from 3; permission conveyed through Copyright Clearance Center, Inc."

An ES is composed of two electrodes containing an active material, a binder and often a conductive material to boost the conductivity. Both electrodes are immersed in an electrolyte assuring the ion transport, an insulator separator is used to prevent short circuits and the whole is connected to two current collectors from the two parts (Figure 2).

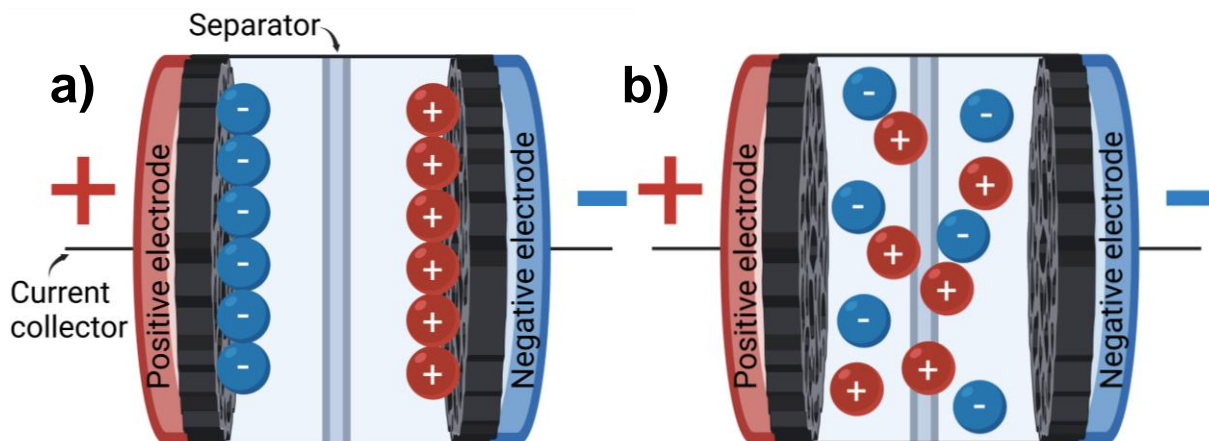


Figure 2 Scheme of an electrochemical capacitor in both (a) charged mode (b) discharged mode. Created by authors using BioRender software.

In laboratory research, several types of 2 electrode cells/devices are used. The most employed ones are Swagelok<sup>6</sup>, coin<sup>7</sup> and pouch<sup>8</sup> cells. One should be aware that each of these systems has different characteristics: dimension, type of current collector, etc. Therefore, the resistivity for each type of cell is different, and this has a direct impact on performance.<sup>9</sup>

## II.2. Mechanisms of energy storage

Depending on the charge storage mechanism, two main types of ES are outlined, namely electrochemical double-layer capacitors (EDLC) and pseudocapacitors.

### II.2.1. Electrochemical double layer capacitors (EDLC)

As noted above, the concept of EDL was introduced by the Helmholtz model (Figure 3), in which electrolyte ions form a charged ionic layer closely adjacent to the electrode surface charged oppositely. This simplest model was further improved by the Gouy-Chapman model, suggesting that the ions present at the electrode-electrolyte interface tend to diffuse within the liquid phase and their dynamics determines the thickness of the diffusive layer. Nevertheless, this model fails to describe the strongly charged EDL. The Stern model suggested the combination of both previously mentioned models, namely the presence of a static Helmholtz layer (or Stern layer) adjacent to the electrode surface and an external Gouy-Chapman layer.

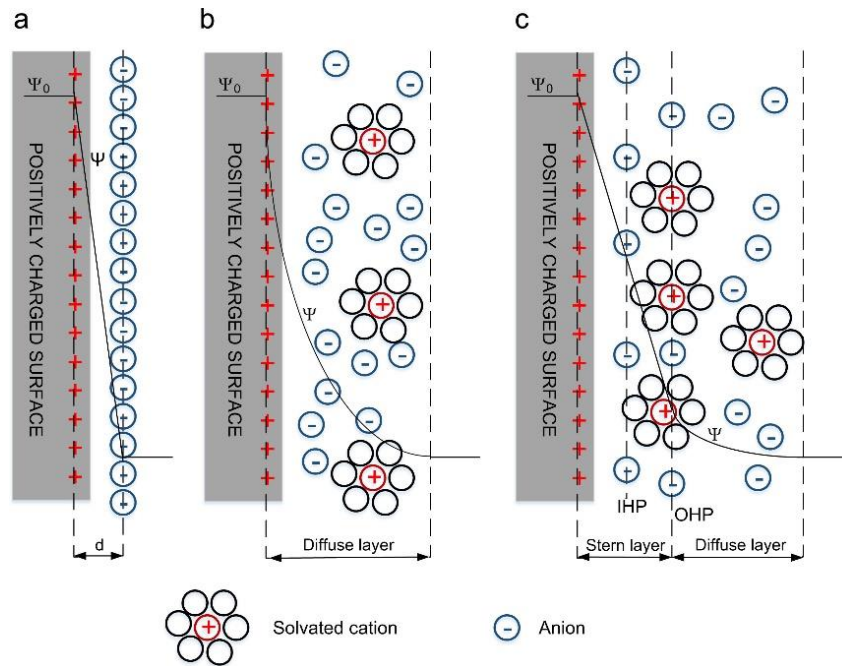


Figure 3 : EDL models ,(a) Helmholtz model, (b) Gouy–Chapman model, and (c) Stern model. Reprinted from 5, with permission from Elsevier.

The short thickness of the EDL,  $d$  1-2 nm (in concentrated solutions) and the high solvent dielectric constant (in aqueous solutions,  $\epsilon \approx 80$ ), results in a relatively high interfacial capacitance  $C_s$  5-20  $\mu\text{F}/\text{cm}^2$ , much higher than one of the electrostatic capacitors (hence is the term “supercapacitors”). The small thickness of EDL also allows using rough or porous electrodes with high SSA. In particular, the carbon electrodes with  $\text{SSA} > 2500 \text{ m}^2 \text{ g}^{-1}$  are often used in ES (see III.3), thus providing high mass specific capacitance of the device  $C_m$  above 100  $\text{F g}^{-1}$ .

The decrease of the pores of the material allows its SSA to increase without a strong decrease in its density, resulting in high values of both  $C_s$  and  $C_V$ . In fact, an increase in mass specific capacitance  $C_m$  is observed with an increase in  $\text{SSA}^{10}$  in a wide range of SSA from below 1000  $\text{m}^2 \text{ g}^{-1}$  up to  $\text{SSA} > 2500 \text{ m}^2 \text{ g}^{-1}$ . However, the detailed analysis of numerous literature data <sup>11</sup> suggested a decrease of surface-specific capacitance  $C_s$  of carbon electrodes from ca. 14  $\mu\text{F cm}^{-2}$  at  $\text{SSA} < 1000 \text{ m}^2 \text{ g}^{-1}$  to ca. 5  $\mu\text{F cm}^{-2}$  at  $\text{SSA} > 2500 \text{ m}^2 \text{ g}^{-1}$ . These discrepancies might be related to an inaccessible porosity (pore size not matching the electrolyte one) or due to other factors (conductivity etc.).

The Stern model gives correct description of EDL of flat uniform electrodes, but is less capable to describe the electrosorption of ions within the electrode micropores with diameter comparable to EDL thickness. In such case the EDL of opposite walls are overlapping, which may result in a decrease of  $C_s$ .



More recently, new in situ characterization tools, for instance, nuclear magnetic resonance (NMR), Raman spectroscopy, and X-ray scattering, have been used to deepen the understanding of ion mobility within the pores. Furthermore, electrochemical quartz-crystal microbalance proved to be a powerful technique in revealing electrolyte dynamics and ion adsorption during polarization.<sup>12</sup> Parallel to experimental techniques, modeling answered several questions not achievable by experimental procedures.<sup>13</sup> Studies using Carbide-derived carbon (CDC) with narrow pore size distribution,<sup>14,15</sup> have been used in several studies and demonstrated an increase in  $C$  when the diameter of the pores  $d_p$  becomes small and comparable with the size of the ions of the electrolyte  $d_i$  depending on the electrolyte/solvent system. Thus, complex dependence of  $C_s$  on  $d_p$  has been suggested, with the maximum  $C_s$  at ca.  $15 \mu\text{F cm}^{-2}$  in ionic liquids, or  $10\text{-}12 \mu\text{F cm}^{-2}$  in organic electrolytes,<sup>16</sup> and in aqueous electrolytes<sup>11</sup> for pores with size  $d_p \approx d_i$  ( $d < 0.7 \text{ nm}$ )<sup>10,17,18</sup>.

It should be mention that there is no full consensus on this complex  $C_s$ - $d_p$  dependence: a constant value of  $C_s$  inside of micropores has also been recently suggested.<sup>19</sup> The unambiguous interpretation of experimental data is complicated due to (i) a certain broadness of pore size distributions even for model 3D carbon materials, such as CDC and (ii) difficulties in interpretation of BET isotherms especially in the case of micropores. However, it is generally accepted that pore sizes that match the size of electrolyte ions proved to be the best pore geometry.<sup>20,21</sup> It is also argued that mesopores (pores wider than  $2 \text{ nm}$ )<sup>22</sup> have been argued to improve ES performance, as they assure rapid access of electrolyte ions to micropores. The geometry and connectivity of mesopores are also of great importance to enhance diffusion and capacity retention.<sup>23</sup>

### II.2.2. Pseudocapacitors

Pseudocapacitance is a phenomenon of interfacial charge storage involving a faradaic (charge transfer) reaction, contrast pure electrostatic adsorption in the case of EDL formation<sup>24</sup>. The term 'pseudo'-capacitance is justified by a signature behavior (cyclic voltammetry (CV) or galvanostatic charge-discharge (GCD) of pseudocapacitors similar to EDLC, showing only a weak dependence of capacitance on potential. Generally speaking, pseudocapacitance occurs when fast reversible faradaic reactions arise at or near the surface of an electrode material<sup>25</sup>, resulting in charge accumulation in the interfacial region. For a deeper understanding, the historical evolution of pseudocapacitance definition is nicely summarized in the literature.<sup>25,26</sup>

The use of pseudocapacitance in ES emerged with the report of Trasatti et al. in 1971, on highly reversible charge transfer reactions for hydrous ruthenium oxide  $\text{RuO}_2$ .<sup>27</sup> It exhibited symmetric and reversible CV that was explained by reversible redox reactions later on in 1990.<sup>28</sup> Other reports revealed that nanoscale structure contributes to enhance the performance, a capacitance of  $700 \text{ F g}^{-1}$  being reached.<sup>29</sup> Since ruthenium is rare and high cost material, there was a sparkling interest to find low-cost and abundant metal oxides that show similar behavior. Goodenough *et al.* reported in 1999 capacitive behavior for amorphous hydrated  $\text{MnO}_2$  in neutral aqueous electrolytes (2 M KCl).<sup>30</sup> The specific capacitance was lower ( $\sim 200 \text{ F g}^{-1}$ ) than  $\text{RuO}_2$  in a potential window of 0 V to 1.2 V. Although  $\text{MnO}_2$  has lower electrical conductivity, it attracted interest due to its capacitance and economic affordability. To date,  $\text{MnO}_2$  has become one of the most studied pseudocapacitive materials.

Later on in 1999, Conway suggested 3 major categories of faradaic mechanism of charge storage<sup>31</sup> (Figure 4): (a) underpotential deposition, i.e., deposition of a monolayer of adsorbed ions accompanied by charge transfer; it is also called adsorption pseudocapacitance (b) redox pseudocapacitance that takes place when ions are involved in a faradaic reaction with electrode material and (c) intercalation pseudocapacitance that occurs by intercalation of ions into the surface and sub-surface layers of a host material, accompanied by charge-transfer reactions but no crystallographic phase change (contrary to batteries).

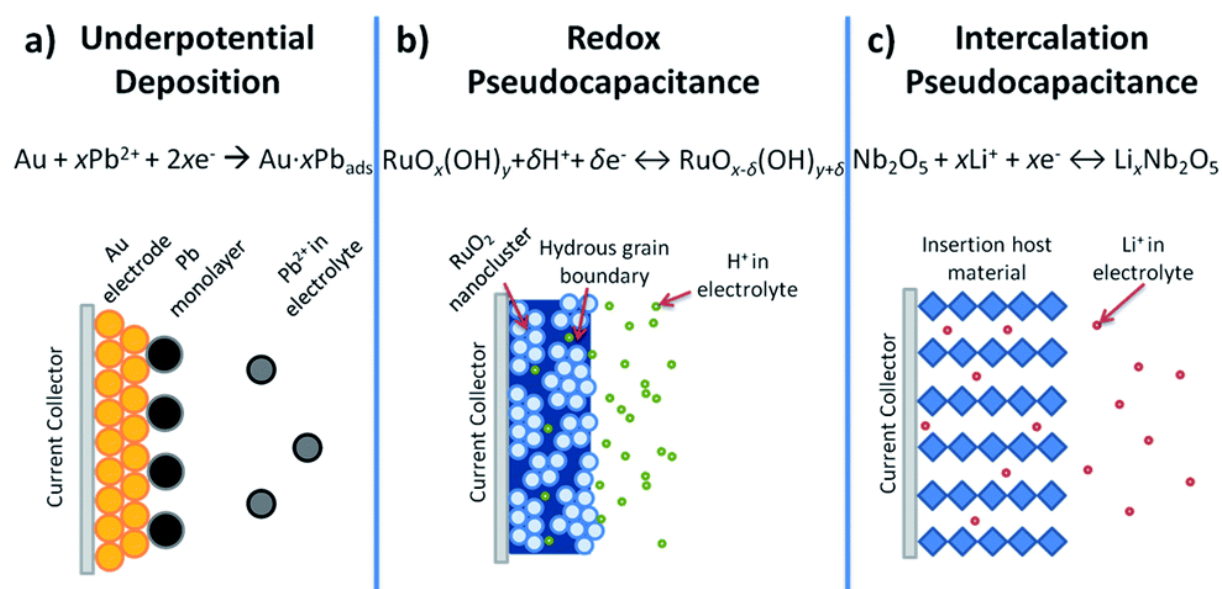


Figure 4 : Different types of pseudocapacitance mechanisms: (a) underpotential deposition (b) redox pseudocapacitance (c) intercalation pseudocapacitance. Used with permission of Royal Society of Chemistry, from<sup>25</sup> ; permission conveyed through Copyright Clearance Center, Inc.

Obviously, the shape of the electrochemical signatures is different depending on the type of pseudocapacitance and many other factors, such as the size and shape of the particles within the electrode, and the respective interaction of the electrode with the electrolyte.<sup>20</sup> Nanostructuring plays an important role in pseudocapacitance as it controls the transport of ions within the material. In some cases, typically for materials that have faradaic charge storage via ion insertion (Fig.4c), the CV and GCD shape are closer to battery-type insertion materials<sup>32</sup>, but show more reversible behavior due to a shorter ion diffusion distance achieved by nanostructuring of the material. This manifests itself in an appearance of pseudocapacitance and is considered extrinsic pseudocapacitance.<sup>26</sup> For example,  $\text{Nb}_2\text{O}_5$  was tested as nanoscale material and showed an intercalation pseudocapacitance which do not appear for bulk  $\text{Nb}_2\text{O}_5$ <sup>33</sup> (Fig.5). This was defined as extrinsic pseudocapacitance. In addition to this example, other materials such as  $\text{V}_2\text{O}_5$ <sup>34</sup> and  $\text{TiO}_2$ <sup>35</sup>  $\text{LiCoO}_2$ <sup>36</sup> showed pseudocapacitance when nanostructured.

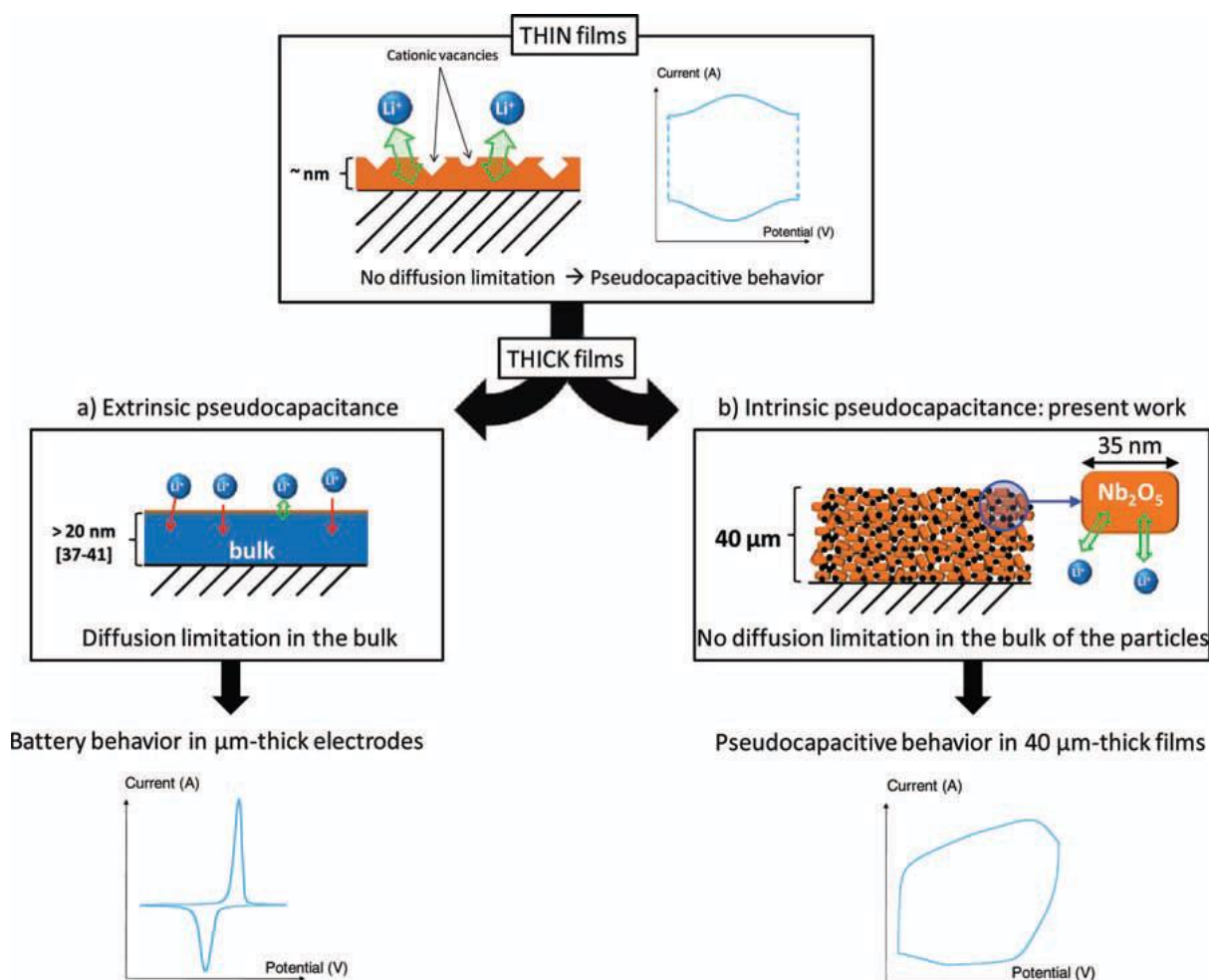


Figure 5 Schematic representations and corresponding electrochemical responses for 'extrinsic' and 'intrinsic' pseudocapacitors. <sup>33</sup> Reproduced by permission of IOP Publishing Ltd.

Generally, pseudocapacitive materials possess higher theoretical capacitance than EDL materials.<sup>37</sup> Hence, they are promising to develop high energy and power devices. However, their large utilization is often impeded by their limited conductivity and low cycling stability, consequently their improvements still require significant attention.

### II.3. Types of supercapacitors

As has been demonstrated before, the nature of the electrode mainly defines the mechanism of energy storage. Thus, electrode materials of EC can be classified by the mechanism of energy storage as EDL capacitors and pseudocapacitors. Alternatively, supercapacitor devices can be classified by their configuration as symmetric, asymmetric, and hybrid supercapacitors.

#### II.3.1. Symmetric supercapacitors

Symmetric capacitors are intensively studied due to the simplest approach to building a capacitor and interpreting performance.<sup>38</sup> In a symmetric supercapacitor, the nature of active material in the positive and negative electrodes is the same. The equivalent circuit of this configuration is depicted in Figure 6, assuming that each electrode behaves as a capacitor  $C_1$ . The performance of the device depends on both  $C_1$  and  $R$  – equivalent serial resistance of the device. Figure 6 shows how the shape of CV curves (Figure 6A) and GCD curves (Figure 6B) changes with an increase in  $R$ , assuming that the value of  $C$  is potential independent. As  $R$  increases, the area under both CV and GC curves, proportional to the capacitance of the device, decreases, especially for fast charging rates.

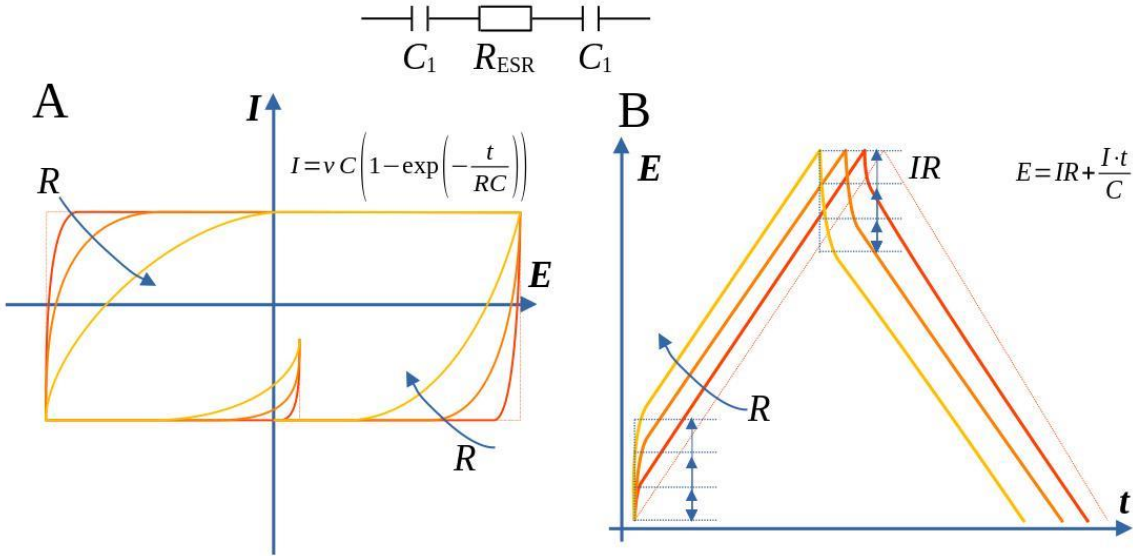


Figure 6 Schematic illustration of the changes in the shape of CV curves (A) and galvanostatic charging curves (B) with increasing serial resistance,  $R$ . The capacitance of an electrode material is assumed to be potential independent for a simplicity.

In many studies, the performance of electrode materials are determined in 3-electrode configuration by using relatively low loadings of material, below  $1 \text{ mg cm}^{-2}$ . Utilization of thin deposits in the model studies allows one to avoid strong resistance of electrode deposit and to demonstrate high specific capacitance of a given electrode material under the optimal conditions. On the other hand, a higher mass loading (ca.  $10 \text{ mg cm}^{-2}$ ) of electrode material is generally required in symmetric supercapacitors<sup>32</sup> to maximize the mass of active components for charge storage. For this high loading, the electrode material contributes ca. 30% of the total mass of capacitor, which makes the specific capacitance of the device ca. three times lower than the capacitance of the electrode material.

An increase in the loading of electrode materials often results in a decrease in the energy capacitance and power density of the supercapacitor, as a thicker electrode layer has higher resistance. Furthermore, to form a stable and uniform thick layer (few hundreds of  $\mu\text{m}$ ), a structuring binder (PVDF most commonly) is added, which can further increase electrode resistance and decrease electrolyte accessibility. The optimization of the composition and the structure of the electrode, as well as the conditions of its formation, have the same importance as a search for the most performing electrode material<sup>39</sup>.

In symmetric supercapacitors, the open circuit potential ( $E_{\text{OCP}}$ ) on both electrodes is the same, and open circuit voltage of the device  $V_{\text{OCP}}$  is 0V (Figure 7). Charging the symmetric supercapacitor results in the same absolute shift of the potential of positive and negative electrodes (but in the opposite directions). Thus, the maximal voltage of the symmetric supercapacitor  $V_{\text{max}}$  depends on  $E_{\text{max}}$ , that is, the closest position of the  $E_{\text{OCP}}$  of the electrode material relative to the positive or negative limits of its potential stability range  $V_{\text{max}} = 2 E_{\text{max}}$ . The optimal electrode/electrolyte system for symmetric supercapacitor has a position of its  $E_{\text{OCP}}$  close to the middle of the potential range of stability of the electrode material.

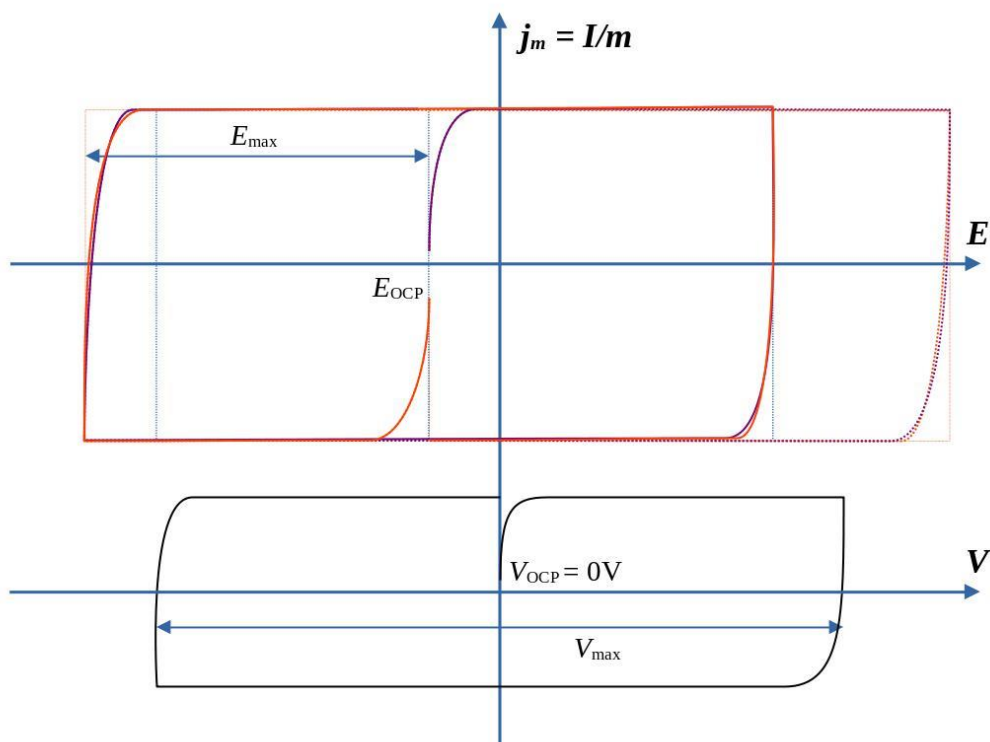


Figure 7 Schematic CV curves of electrodes in symmetric supercapacitors (top) and of the whole symmetric supercapacitor device (bottom). The CV curves of each electrode are shown for 3-electrode configuration (dashed), when the potential of each electrode is controlled by applied voltage

Electrode materials widely used in a symmetric capacitor are carbonaceous ones.<sup>2</sup> Symmetric devices based on pseudocapacitive materials are also developed, but to a lesser extent.<sup>40</sup> In general, carbon materials are considered to be electrochemically stable and inert,<sup>41</sup> allowing them to operate in a wide potential window, mostly limited by the potential range of stability of solvent: from 0.00 V to 1.23 V RHE (Reversible Hydrogen Electrode) for aqueous electrolytes. Moreover, carbon is a poor catalyst of hydrogen evolution and, thus, tolerates voltage below 0.00 V RHE, allowing over polarization of carbon when it is utilized as a negative electrode. However, carbon is thermodynamically unstable and is electro-oxidized above 0.204 V RHE.<sup>42</sup> Its oxidation is kinetically hindered, but, nevertheless, does not allow applying too high positive potentials. Thus, in aqueous electrolytes, the generally accepted operational potential range of carbon electrodes is ca. 1.20 V.

In the absence of any redox system in the electrolyte and specific adsorption of the electrolyte components on the electrode, the value of  $E_{OCP}$  is determined by the value of the potential of zero free charge  $E_{PZC}$ .<sup>43</sup> The value of  $E_{PZC}$  of the graphite electrode in neutral solution is relatively negative (-0.125 V SCE in KF solution),<sup>44</sup> while for more oxidized carbon samples, positive values are reported (ca. 0.090 V SCE in KCl for glassy carbon electrode, for

example<sup>45</sup>). On the other hand, the value of  $E_{PZC}$  can be strongly modified by surface functionalization.<sup>46</sup> Thus, surface treatment of carbon electrode materials allows optimizing its utilization in electrodes of symmetric supercapacitors for a given electrolyte. Nevertheless, the maximal voltage range of operation of symmetric supercapacitors cannot exceed the potential range of operation of electrode materials, e.g. ca. 1.2 V for an aqueous electrolyte.

Considering a symmetric device construction, the mass, thickness, and size of both electrodes should be equal in order to speak about symmetry. Reporting this to Eq. (4), one can conclude that:

$$C_{device} = \frac{1}{2} C_{electrode} \text{ Eq. (5)}$$

Considering  $m_{tot}$  and  $m_{elec}$  the mass of total active material in the device and in one single electrode, and neglecting the mass of other components, a relationship between the specific capacitance  $C_m$  of a device and of a single electrode can be expressed:

$$C_{m,device} = \frac{C_{device}}{m_{tot}} = \left( \frac{C_{electrode}}{2} \right) \cdot \left( \frac{1}{2 \cdot m_{elec}} \right) = \frac{C_{m,electrode}}{4} \text{ Eq. (6)}$$

When electrochemical metrics are reported in the literature, the calculation methods should be given with all the details, formulas, and units to avoid any confusion. Many reported documentation have been proposed<sup>32,47-49</sup> in this direction, with the aim of distinguishing misunderstandings and clarifying the appropriate electrochemical performance metrics. The main difficulties come from the lack of performance standardization in this field.

Despite these limitations, symmetric supercapacitors have certain advantages compared to other types of supercapacitors. Symmetric supercapacitors are easier to optimize, as the same amount of electrode materials is required. Moreover, the polarisation of symmetric supercapacitors can be safely inversed without risk of electrode damage.

### II.3.2. Asymmetric supercapacitor

Asymmetric supercapacitors are used in a wide variety of devices using dissimilar materials in each electrode. Electrodes could be EDL or pseudocapacitive materials.<sup>50</sup> There is some confusion in the identification of capacitors through the literature, as the term asymmetric has been used for a long time, and for any non-symmetric device. Brousse *et al.* gave a clear distinction between pseudocapacitors, asymmetric capacitors and hybrid supercapacitors:<sup>24</sup> according to their definition, asymmetric supercapacitors consist of electrode materials

exhibiting capacitive or pseudocapacitive mechanisms, or even having the same mechanism storage but different mass loading, or surface functional groups.<sup>50,51</sup> Consequently, the term hybrid should be used when a battery type electrode material is used with another type of electrode,<sup>24</sup> either capacitive or faradaic. According to this, hybrid supercapacitor may be seen as a particular type of asymmetric capacitors.

The high loading requirements and, thus, the importance of fabrication of thick, uniform, stable electrode with structure easily accessible for an electrolyte are similar to the electrodes of symmetric supercapacitors. However, utilization of different materials for negative and positive electrodes in asymmetric supercapacitors allows operating wider voltage range compared to symmetric supercapacitors.

The open circuit voltage of the asymmetric supercapacitor  $V_{\text{OCP}}$  is determined by the difference between  $E_{\text{OCP}}$  of positive and negative electrodes. Adjustment of the properties and the amount of materials on the two electrodes allows to utilize the whole potential range of both electrodes: In this case, the maximal voltage  $V_{\text{max}}$  is determined by the difference between the lower potential limit of the negative electrode and the higher potential limit of a positive electrode (Figure 8), and can significantly exceed the stability potential range of each of the electrode material. As each of the electrodes operates in a limited potential range, the degradation of materials can be avoided while maintaining a wide operation voltage of the whole device. This is especially important for oxide electrode materials, which show high specific capacitance but in a rather limited potential range. The choice of electrode material is crucial for the operating potential window of the asymmetric supercapacitors.

The asymmetric pseudocapacitors mentioned in the literature include either a positive pseudocapacitive electrode and a negative capacitive electrode composed of carbon or a positive and negative electrode both composed of pseudocapacitive materials but with different redox reactions (Table 1). As can be seen, the use of carbon as negative electrode is frequently preferred because it offers a low-cost material that has high conductivity and specific surface area, which will boost the asymmetric supercapacitor performance. Moreover, operating carbon as a negative electrode allows to avoid the oxidative degradation of carbon materials at high potentials.



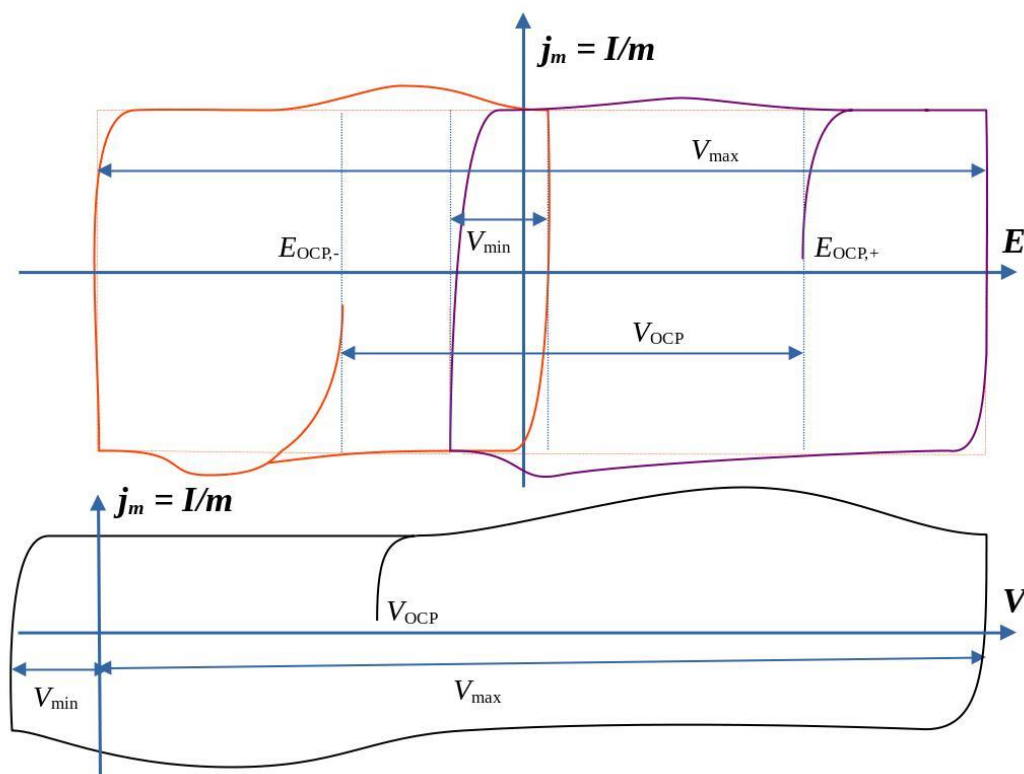


Figure 8 Schematic CV curves of asymmetric supercapacitor: dependence on the potential  $E$  of each of electrode (top), and on the voltage  $V=E+ - E-$  of the supercapacitor (bottom), where  $E+$  and  $E-$  are the potentials of positive and negative electrodes correspondingly.

Some transition metal oxides (TMO) can also operate as negative electrodes in an electrode potential range close to 0.00 V RHE, as illustrated by E-pH Pourbaix diagrams (Figure 9): namely, oxides of Fe (Figure 9A)<sup>52</sup> in basic electrolytes, oxides of V (Figure 9B) in weak acidic or neutral electrolytes, trioxide of tungsten  $WO_3$  in acid electrolytes.<sup>53</sup> On the other hand, oxides of Co, Ni, and especially Mn (Figure 9C) and Ru (Figure 9D) are considered promising positive electrode materials due to redox transitions and intercalation occurring at high potentials.<sup>52</sup> Except for  $RuO_2$ , the other oxides have relatively high electrical resistance and conductive additive, most commonly carbon is necessary, especially to build thick electrode deposits. However, carbon materials are less stable at these high potentials, especially in the presence of metal oxides, which can catalyze their oxidative degradation.<sup>39</sup> In general, highly conductive and stable carbon materials, such as graphitized carbon blacks, are utilized.

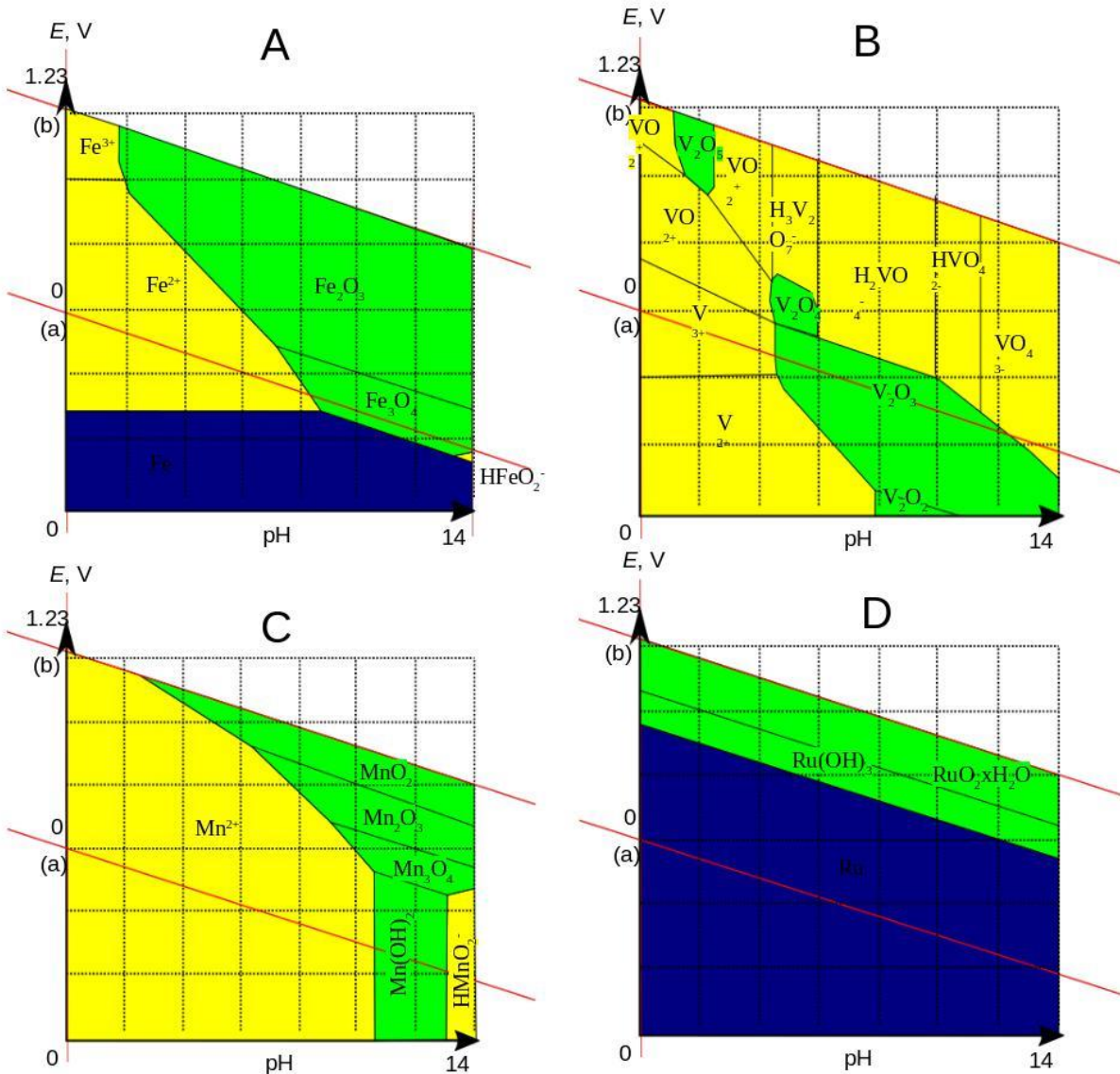


Figure 9 Pourbaix diagrams of some of TMO. Blue fields denote the range of stability of metallic phase, i.e. thermodynamic corrosion immunity. Yellow fields show the range of stability of soluble metallic component, i.e. the thermodynamic range of active corrosion. Green fields show the ranges of the stability of metal oxide phases, i.e. the thermodynamic range of metal passivation. The redox transitions within the green fields are of particular interest for pseudocapacitors.

For the case where two pseudocapacitive materials are used, the most important criteria is to choose them properly according to their standard potential value in the electrolyte.<sup>54</sup>

As seen from the table, the extension of the voltage window for asymmetric capacitors is achieved while using liquid electrolytes (1.7 – 2 V) unlike for symmetric capacitors (~1 V).<sup>61</sup> Consequently, the energy density can be improved without any need to modify the nature of the electrolyte.<sup>62</sup> It is worth mentioning that the value of current density at which the device is tested may affect its retention capacity after certain cycles. Thus, this aspect needs to be taken under consideration when comparing different values.<sup>63</sup>

Table 1: Comparison of selected electrode materials and performance for aqueous capacitive asymmetric supercapacitors.

Positive electrode	Negative electrode	Electrolyte	Voltage window	Capacitance	Energy density	Power density	Retention (cycles)	Refs.
MnO <sub>2</sub>	Activate carbon	2 M KNO <sub>3</sub>	2 V	140 F g <sup>-1</sup> at 0.1 A g <sup>-1</sup>	21 W h kg <sup>-1</sup>	123 kW kg <sup>-1</sup>	NA	55
MnO <sub>2</sub> -carbon nanotube	Carbon nanotube	H <sub>3</sub> PO <sub>4</sub> -PVA	2 V	18 F g <sup>-1</sup> at 0.267 A g <sup>-1</sup>	42 W h kg <sup>-1</sup>	19.25 kW kg <sup>-1</sup>	98% (500)	56
RuO <sub>2</sub> -graphene	graphene	H <sub>2</sub> SO <sub>4</sub> -PVA	1.8 V	167 F g <sup>-1</sup> at 1 A g <sup>-1</sup>	19.7 W h kg <sup>-1</sup>	6.8 kW kg <sup>-1</sup>	95% (2000)	57
RuO <sub>2</sub> -Laser scribed graphene	Activated carbon	1 M H <sub>2</sub> SO <sub>4</sub>	1.8 V	8.6 F cm <sup>-3</sup> at 500 mA cm <sup>-3</sup>	55 Wh kg <sup>-1</sup>	12 kW kg <sup>-1</sup>	93% (4000)	58
MnO <sub>2</sub> -carbon fiber	Fe <sub>2</sub> O <sub>3</sub> -carbon fiber	LiCl-PVA	1.6 V	91.3 F g <sup>-1</sup> (1.5 F cm <sup>-3</sup> ) at 2 mA cm <sup>-2</sup>	0.55 mWh cm <sup>-3</sup>	139.1 mW cm <sup>-3</sup>	84% (5000)	59
CoO <sub>x</sub> -Ni(OH) <sub>3</sub>	Fe <sub>3</sub> O <sub>4</sub> -reduced graphene oxide	6 M KOH	1.7 V	114 F g <sup>-1</sup> at 1.2 A g <sup>-1</sup>	45.3 W h kg <sup>-1</sup>	7080 W kg <sup>-1</sup>	91.8 (5000)	60
VO <sub>x</sub> -carbon fiber	Vanadium nitride-carbon fiber	LiCl -PVA	1.8 V	1.35 F cm <sup>-3</sup> (60.1 F g <sup>-1</sup> ) at 0.5 mA cm <sup>-2</sup>	0.61 mW h cm <sup>-3</sup>	0.85 W cm <sup>-3</sup>	87.5% (10000)	61

PVA: Poly Vinyl Alcohol

Limiting the potential operation range for each of the electrodes allows us to avoid degradation of electrode material. However, tuning and maintaining asymmetric supercapacitors is significantly more challenging. The inversion of the polarizability of the asymmetric supercapacitor above  $V_{\min}$  is critically damaging for electrode materials. The amount of electrode material at both electrodes must be equilibrated to ensure the maximal operating voltage without overstepping the safe potential operating range. However, the most challenging part is the management of performance retention. Faster degradation of the material of one of the electrodes results in its stronger polarizability under the same voltage, which may cause its even faster degradation.

## III. Electrode materials

### III.1. Carbon Materials

Carbon materials are the most commonly used class of materials in supercapacitor electrodes. A predominant part of supercapacitor market is occupied by EDLC, in which carbon are the main component of electrodes.<sup>64</sup>

There are several advantages of using carbon-based materials as electrodes in electrochemical energy storage devices.

- Carbon is the 12<sup>th</sup> most abundant element on Earth<sup>65</sup>, and can be synthesized from various fossil and biomass sources.
- Carbon has the lowest electrical resistance among all nonmetal elements. The in-plane resistivity of graphite is  $0.4 \mu\Omega \text{ m}^{66}$ , which is just a few times higher than the typical resistivity of transition metals (e.g.  $0.096 \mu\Omega \text{ m}$  for Fe). The conductivity of carbon is provided by the  $\pi$ - $\pi$  electrons in ordered carbon sheets  $sp^2$ . The conductivity of carbon materials is related to the ratio of  $sp^2$  and  $sp^3$  carbon, as well as to the size of ordered  $sp^2$  domains. The conductivity of carbon materials spans from about  $105 \Omega^{-1} \text{ cm}^{-1}$  for the defect-free graphene sheet to ca.  $10\text{-}15 \Omega^{-1} \text{ cm}^{-1}$  for the diamond.

The apparent conductivity of powdered carbon materials depends on the intrinsic resistivity of carbon and the intergranular resistance of the carbon particles. In general, more compact materials (i.e. carbon materials with higher apparent density) have higher conductivity due to lower intergranular resistance<sup>67</sup>; compressing porous activated carbon results in many times (3-10 times) increase of its apparent conductivity.<sup>68</sup>

- An important advantage of carbon materials is their versatile structure. In particular, macro-, micro-, and nanostructures of carbon materials can be varied and adjusted to the best performance. Carbon materials can be prepared in the form of powders, paper-like fibrous tissues, sheets, felts, amorphous strong solids, etc., e.g. in various macrostructures. On the other hand, due to the variability of microstructure, the specific surface area of carbon materials can be varied from ca.  $2.5 \text{ m}^2 \text{ g}^{-1}$  for natural graphite to  $>2000 \text{ m}^2 \text{ g}^{-1}$  for activated carbons<sup>41</sup>.

According to their architectures, carbon materials can be classified as 0D, 1D, 2D and 3D materials.

### III.1.1 0D carbon materials

Carbon nanodots (CND) are a relatively recent class of 0D carbon materials with a characteristic size of carbon particles or sheets below 10 nm.<sup>69</sup> CND can be synthesized by controlled strong oxidation (thermal, thermochemical, or electrochemical) of graphitic carbon, resulting in exfoliation and rupture of graphene sheets, producing nanoparticles or nanosheets of graphene with oxidized carbon edge atoms. Alternatively to this top-down approach, CND can also be synthesized by bottom-up approach from organic precursors.<sup>70,71</sup>

The small size of the carbon domains and the strong influence of the carbon atoms on the edges result in a disruption of  $\pi$ - $\pi$  electrons conjugation. Below a certain size (few nm) small CND are becoming semiconducting quantum dots (CQD),<sup>45</sup> which attract little interest for energy storage applications due to limited conductivity. However, CND is studied as an interesting system for the supercapacitors electrode as a precursor for the 3D porous carbon electrode material<sup>72</sup>, or as an additive to other electrode materials.<sup>73,74</sup> The presence of polar hydrophilic oxygen-containing functional groups at the carbon edges strongly influences the properties of CND. In particular, CNDs are easily dispersible in aqueous solutions. Controlled reduction (thermal, thermochemical, or electrochemical) of oxidized edge carbon results in re-stacking of CND in a 3D porous carbon structure,<sup>75</sup> with similarly high SSA > 1700 m<sup>2</sup> g<sup>-1</sup> as activated carbon (AC). However, CND-derived carbon has a more compact structure, resulting in a higher apparent density, ca. 1 g cm<sup>-3</sup> compared to typical densities of thermochemical AC of 0.3-0.6 g cm<sup>-3</sup>. This results in high mass-specific (270 F g<sup>-1</sup>) and volume-specific (262 F cm<sup>-3</sup>) capacitances in 6 M KOH at 1 A g<sup>-1</sup> detected for high electrode loading of 10 mg cm<sup>-2</sup>.

CNDs are utilized for the functionalization of porous carbon electrode materials.<sup>73,76</sup> The strong hydrophilic nature of CNDs allows better electrolyte accessibility for carbon micropores. This effect is claimed to be particularly strong in the case of N-doped CND.<sup>77</sup> CNDs are also utilized as a building conducting block of composite materials with metal oxide nanoparticles<sup>78</sup> and halide perovskites<sup>79</sup> with high capacitance and electrochemical stability.

High-temperature (above 1200°C) vacuum annealing of nanodiamonds (produced by detonation) results in ca. 10 nm graphitic carbon nanoparticles, consisting of concentric spheres: carbon nanoonions (CNO).<sup>80</sup> Due to its inner graphitic structure, CNO has higher conductivity than CND: apparent conductivity of CNO increases with annealing temperature up to ca. 3  $\Omega^{-1}$  cm<sup>-1</sup>. Furthermore, despite the higher intergranular resistance of CNO, its apparent conductivity is higher than the typical conductivity of activated carbon,<sup>81</sup> which, in general, lacks long

ordered graphitic  $sp^2$  domains. Due to the larger particle size, the SSA of CNO is ca.  $500 \text{ m}^2 \text{ g}^{-1}$ , that is a few times lower than SSA of CND. Thus, the mass-specific capacitance of CNO is not high: generally, the values of ca.  $40\text{-}50 \text{ F g}^{-1}$  are reported. However, chemical functionalization allows increasing capacitance up to  $\sim 100 \text{ F g}^{-1}$ . Nevertheless, lack of micropores in dense CNO deposit and its high conductivity make it an interesting material for capacitors with high power output.<sup>71,82,83</sup>

### III.1.2. 1D Carbon

Carbon nanotubes (CNT) and nanofibers (CNF) are the most commonly used types of carbon 1D material in supercapacitors, which can be synthesized by various methods.<sup>84</sup> The most commonly used method is chemical vapor deposition by decomposition of hydrocarbon precursors, allowing the preparation of vertically aligned nanotubes (VACNT).

The main advantage of 1D carbon as an electrode material is controlled porosity with predominance of mesopores, especially in the case of VACNT. The geometry and composition of CNT can be finely tuned, which makes CNT a very suitable model material for studying the performance of supercapacitors. Due to their regular and tunable geometry and composition, CNTs and CNFs are often used in composites with conductive polymers and/or metal oxides in supercapacitors.<sup>84</sup>

On the other hand, the disadvantage of CNT is a relatively low SSA (generally less than  $250 \text{ m}^2 \text{ g}^{-1}$ ). Chemical post-treatment may result in an increase in SSA up to ca.  $500 \text{ m}^2 \text{ g}^{-1}$  and functionalization of the carbon surface by O- and N-containing groups,<sup>85</sup> providing mass-specific capacitance of  $\sim 200 \text{ F g}^{-1}$ .

### III.1.3 2D Carbon

Graphene is the 2D carbon material, which consists of separated (exfoliated) sheets of  $sp^2$  carbon. This material has high mechanical stability: the Young modulus of the defect-free single graphene sheet is equal to 1.0 TPa, its breaks stress is 130 GPa.<sup>86</sup> Graphene has high theoretical SSA of  $2628 \text{ m}^2 \text{ g}^{-1}$ .<sup>87</sup> The single sheet of graphene has relatively low electrical surface electrical resistance  $400 \text{ Ohm sq}^{-1}$ , which is decreased to ca.  $30 \text{ Ohm sq}^{-1}$ . for the film of 4 stacked graphene sheets with ca. 2 nm stack thickness.<sup>88</sup> The bulk conductivity of such a graphene-type film is estimated to be  $1.6 \cdot 10^6 \text{ Ohm}^{-1} \text{ cm}^{-1}$ .

The high electronic conductivity and mechanical stability make graphene a very attractive electrode material for EDLC. Moreover, on the basis of experimental data for graphene deposits

on flat Cu substrate and molecular dynamics simulations, high surface capacitance (ca.  $13.5 \mu\text{F cm}^{-2}$ ) of a single graphene sheet has been argued,<sup>89</sup> which decreases to approximately  $5 \mu\text{F cm}^{-2}$  with increase of graphene stack thickness. Thus, the mass-specific capacitance of an electrode material composed of single sheet graphene is expected to provide maximal theoretical capacitance of  $355 \text{ F g}^{-1}$ . However, there are two main challenges of graphene utilisation as an electrode material: (i) the tendency of restacking of graphene sheets upon deposition on the electrode, and (ii) the cost of graphene synthesis scaled up to the quantities above laboratory needs.

The methods of graphene synthesis are typically divided into 2 groups: top-down methods (e.g. mechanical exfoliation, chemical and sonochemical exfoliation) and bottom-up methods (e.g. chemical vapor deposition, CVD). The CVD and mechanical exfoliation allow one to produce high quality graphene films<sup>75</sup>, however, their application is limited to nonporous substrates. Moreover, among the top-down methods, mechanical exfoliation is the most difficult to scale up. Alternatively, the chemical exfoliation route can be easily scaled up to mass production. The two most common strategies for chemical exfoliation are sonochemical exfoliation and the chemical route (Hummer method<sup>90</sup> and its derivatives<sup>91</sup>).

The sonochemical exfoliation of graphite is based on the presence of an exfoliating chemical agent in the sonicated liquid dispersion of graphite. The most typical efficient exfoliating agents are polycyclic aromatic hydrocarbons, pyrene derivatives, or certain polymers.<sup>92</sup> The variety of exfoliation agents allows to form stable aqueous and organic dispersions of partially stacked graphene sheets, most commonly with few (less than 10) layers stacked. Thus, the resulting materials are commonly referred to as few-layer graphene (FLG). In recent years, the utilization of biocompatible surfactants, such as oligopeptides<sup>93</sup> tannic acid<sup>94</sup> is proposed for preparation of a stable aqueous dispersion of FLG.

The first step of the chemical route consists of the chemical oxidation of graphite; resulting in efficient exfoliation of graphene sheets and formation of graphene oxide (GO). The oxygen containing functional groups introduces repulsive interaction between GO sheets. The hydrophilic nature of GO sheets facilitates oxidative exfoliation of graphite in aqueous solutions, resulting in stable water suspension of GO. The next step is the reduction of GO, either thermally at a temperature above  $750^\circ\text{C}$ , or chemically by  $\text{NaBH}_4$ ,  $\text{N}_2\text{H}_4$ , or electrochemically<sup>76</sup>, and the formation of reduced graphene oxide, rGO<sup>95,96</sup>. rGO is a graphene-like material characterized by a relatively high density of structural defects owing to oxidation-induced structural damage and an incomplete reduction of oxidized functional groups.

From the viewpoint of energy storage applications, the additional advantage of the GO / rGO route is that the partially reduced oxygen-containing functional groups can be electrochemically active and thus can add the charge storage capacitance due to the pseudocapacitance.<sup>75</sup> The main challenge of the GO / rGO route is to find the optimal conditions for each of its steps. The typical SSA and the mass specific capacitance of rGO electrode materials are reported in the range of 400-700 m<sup>2</sup> g<sup>-1</sup> and 150-260 F g<sup>-1</sup> respectively.

A comparison of the chemical or electrochemical oxidation/reduction (GO/rGO) route and the sonochemical exfoliation (FLG) demonstrated<sup>97</sup> that the latter generally has lower yield and requires a longer time to prepare a comparable amount of graphene-type material, but results in a less severely damaged final material.

Stand-alone graphene materials (rGO or FLG) are rarely utilized in supercapacitors due to the re-stacking tendency and limited accessibility of the carbon surface in the presence of surfactants.<sup>81</sup> To avoid re-stacking, spacers are introduced between graphene sheets: for example, CNT<sup>98,99</sup> or metal nanoparticles.<sup>89</sup>

An alternative approach is the introduction of structuring compounds, i.e. template synthesis, in the thermal annealing step. Polymers, metals, or metal oxides are commonly applied as templates.<sup>75</sup> The resulting materials have high conductivity due to graphitic, or FLG core structure, and high SSA and open controlled porosity due to the presence of structuring components. The electrode consisted of graphene/PANI foam with loading of 0.90-0.96 mg cm<sup>-2</sup> demonstrated an outstandingly high mass-specific capacitance of 790 F g<sup>-1</sup> in 1 M H<sub>2</sub>SO<sub>4</sub> at 1 A g<sup>-1</sup>. This high capacitance is above the theoretically predicted value of the stand-alone graphene sheet (ca. 550 F g<sup>-1</sup>), indicating the contribution of PANI.

Inorganic templates, most commonly SiO<sub>2</sub>, MgO or Mg(OH)<sub>2</sub>, are also used to control the carbon structure during thermal reduction of graphene.<sup>17,100</sup> Carbon thermochemical activation by KOH in the presence of NaCl as an inorganic soluble template has been demonstrated to produce porous layered carbon with FLG core structure,<sup>18</sup> and the thickness of FLG stacks of few tens of graphene sheets. This carbon has a relatively developed surface area (630-890 m<sup>2</sup> g<sup>-1</sup>) and a high mass specific capacitance of 293 F g<sup>-1</sup> (i.e. ca. 38 μF cm<sup>-2</sup>) at 1 A g<sup>-1</sup> in 0.5 M H<sub>2</sub>SO<sub>4</sub>. Only moderate decrease in specific capacitance to 230 F g<sup>-1</sup> (ca. 30 μF cm<sup>-2</sup>) observed when the charging rate is increased to 50 A g<sup>-1</sup>, demonstrating the faster pseudocapacitance phenomenon.



### III.1.4. 3D Carbon

The activated carbon (AC) forms the class of 3D carbon materials with the highest experimentally observed SSA, larger than  $3000 \text{ m}^2 \text{ g}^{-1}$ .<sup>46</sup> It is important to recall that the highest SSA of graphene, calculated from the density of carbon atoms in closed-packed  $\text{sp}^2$  layers is  $2628 \text{ m}^2 \text{ g}^{-1}$ . The SSA values above this value suggest an anomalously high utilization of the carbon surface and distortion of the  $\text{sp}^2$  carbon structure.

The other advantage of the activated carbon is relatively straightforward synthesis routines, which can be broadly classified as (i) the physical and (ii) the chemical carbon activation methods using affordable precursors such as biomass.<sup>101</sup>

In both routes, an annealing of carbon precursor material at high temperature, generally above  $600 \text{ }^\circ\text{C}$ , is utilized to transform an initial compact carbon structure into a highly porous one. In the physical activation route the modification is typically done at a temperature above  $800 \text{ }^\circ\text{C}$  in the inert atmosphere (i.e. carbonization), or in the presence of etching gas components, such as the  $\text{CO}_2$ ,  $\text{H}_2\text{O}$  stream.<sup>102</sup> Chemical activation is similar to the physical activation except that carbon modification is assisted by chemical etching agents mixed with the carbon precursor before thermal annealing. The most typical etching agents are  $\text{NaOH/KOH}$ ,  $\text{H}_3\text{PO}_4$ ,  $\text{H}_2\text{SO}_4$ ,  $\text{K}_2\text{CO}_3$ ,  $\text{ZnCl}_2$ . The temperature at which the resulting carbon material has the highest SSA depends on the source of carbon. For example, a detailed study of the activation of pine-derived biomass<sup>102</sup> demonstrated that the highest surface area of BET was obtained after pyrolysis at  $600\text{-}800^\circ\text{C}$ , while a further increase in temperature resulted in a sharp decrease in surface area.

Thermochemical activation of carbon results in carbon materials with a strong contribution of micropores and a high SSA above  $2000 \text{ m}^2 \text{ g}^{-1}$ . This high SSA results in mass-specific capacitance  $C_m$  above  $200 \text{ F g}^{-1}$  routinely reported for AC carbon materials.

Various sources of carbon have been used for the preparation of AC using the chemical activation method. The utilization of natural, abundant, and cheap carbon sources, such as peat, wood, biowastes, wastes, or agricultural wastes attracted strong research interest as a strategy of biomass valorisation.<sup>103,104</sup> The chemical activation of a biosource precursor eliminates most of the elements other than carbon and creates a porous structure with a well-developed surface area. The structure of the final activated carbon depends on the activation parameters: namely, nature and concentration of an activation agent, temperature, and duration of the activation step.

### III.2. Carbon/ transition metal oxide composites

Transition metal oxides (TMO) are attractive as a supercapacitor electrode, as they have a specific capacitance of one order of magnitude higher than carbon.<sup>105</sup> However, in general, metal oxides alone present some drawbacks while cycling: i) poor conductivity that yields a high resistivity of the device, ii) strain developed during cycling that causes cracking of the electrode, hence poor long-term stability, and iii) a restricted surface area that is difficult to tailor for metal oxides,<sup>106</sup> iv) significant loss of capacitance with an increase in charging rate: For instance, it has been reported that only 23% of NiO capacitance is kept at a sweep rate of 100 mV s<sup>-1</sup> compared to 1 mV s<sup>-1</sup>.<sup>107</sup> All of these inconvenient leads to research efforts to develop new composite materials made from metal oxides and carbon materials. Figure 10 presents current investigation routes to obtain improved electrochemical capacitors.

Composite materials combine the merits of both components and lessen the shortcomings of both. The most used approach is composite engineering with a very conductive material, i.e., carbon. At the same time, it ensures a physical support for the TMO materials and a rapid charge transport<sup>22</sup>, providing a high power density of the device. On the other hand, the presence of metal oxides in the composite provides high capacitance, leading to high energy density of the device. The synergistic effect of the two materials is then expected to boost the key metrics of a supercapacitor.<sup>108</sup> Since the surface area of metal oxides depends strongly on their microstructures,<sup>109</sup> nanostructuration is highly desired. The confinement of TMO in the carbon matrix constitutes a double gain, as the conductivity is improved and the nano effect is preserved during cycling due to the presence of carbon that encloses the particles and prevents their aggregation.<sup>110</sup>

Various metal oxides with different pseudocapacitive mechanisms were reported as electrode materials for supercapacitors : intrinsic pseudocapacitive materials such as RuO<sub>2</sub><sup>112</sup>, MnO<sub>2</sub><sup>113</sup> and battery types materials, that exhibit pseudocapacitance when nanostructured, i.e., V<sub>2</sub>O<sub>5</sub><sup>114</sup>, nickel<sup>115</sup> and cobalt hydroxides<sup>116</sup>. Concerning the morphological control, the synthesis of TMO/carbon nanocomposites has included nanoparticles<sup>110</sup>, nanowires<sup>117</sup>, nanofibers<sup>118</sup>, nanoflakes<sup>119</sup>, nanospheres<sup>120</sup> and other nano-forms.<sup>121</sup> As for the electrochemical performance, TMO/carbon nanocomposites allows increasing the capacitance and/or the voltage window for certain configurations and hence, improving the energy and power density compared to EDLC.

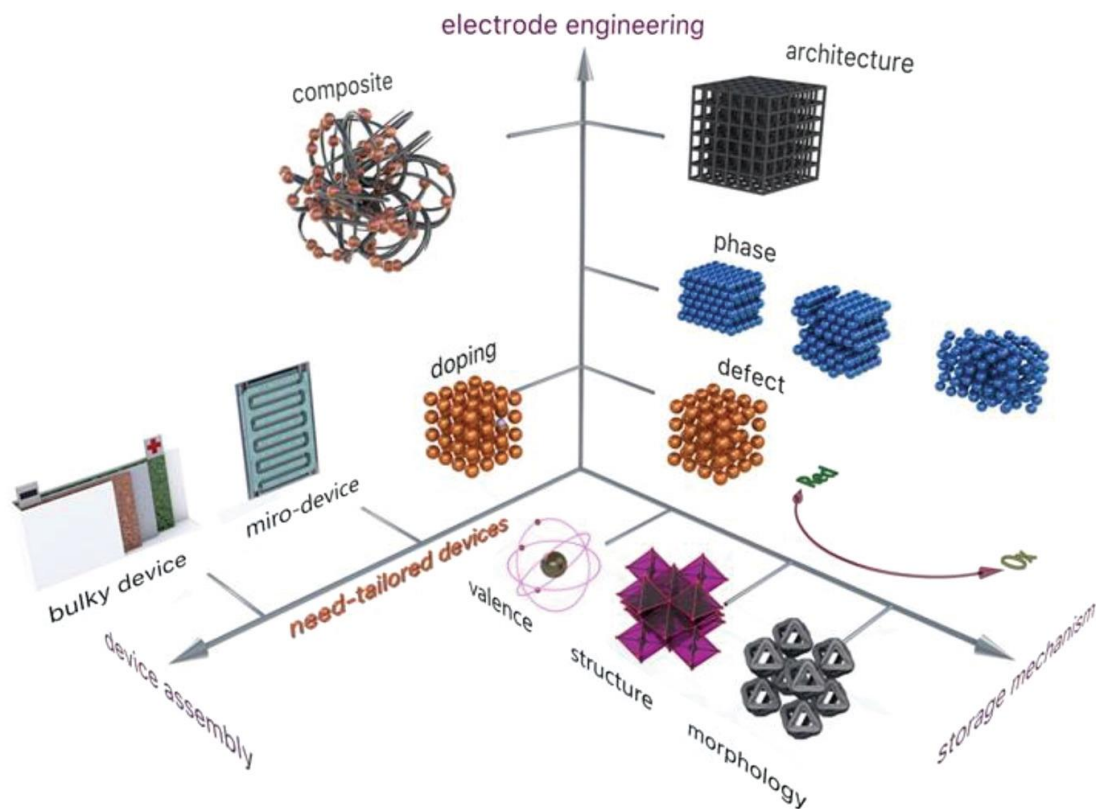


Figure 10: Scheme of relevant research routes for enhanced electrochemical capacitors including charge storage mechanisms, electrode materials engineering, and functional device assemblies. Figure reprinted from <sup>111</sup>

Table 2 presents the electrochemical performance characteristics of different TMO /carbon composites. Many parameters influence capacitance and energy density and one should be aware of the experimental conditions/calculations that might lead to atypical performance.<sup>32,122</sup> In particular, numerous studies report the performance of electrode material measured in the 3-electrode configuration. As explained in II.1, the energy density of a 2-electrode device with the same electrode materials is expected to be at least a few times lower due to the contribution of other components to the device mass/volume. One should keep in mind that the three-electrode system must be used only to study the properties of electrode materials and, in particular, charge mechanisms of electrodes. Moreover, in an asymmetric 2-electrode device, the properties of an electrode material strongly depend on a choice of the opposite electrode (composition and amount) and its energy storage mechanism. Methods of calculation are often mentioned in the literature but still are a source of confusion.<sup>38</sup> Several insightful reports attempted to standardize the good practice of supercapacitor metrics through the last decades.<sup>48,123</sup> These precautions are valid for any type of material and cell, and have to be considered in order to properly evaluate the electrochemical characteristics of electrode materials.

Table 2 : Comparison of carbon/metal oxide composites as electrode materials for supercapacitors.

Electrode material	Electrolyte	Type of cell	Specific capacitance	Specific Energy and Power	Retention (cycles)	Refs
RuO <sub>2</sub> /graphene	0.5 M H <sub>2</sub> SO <sub>4</sub>	2 electrode symmetric	479 F g <sup>-1</sup> at 0.24 A g <sup>-1</sup>	20.28 W h kg <sup>-1</sup> , 600 W kg <sup>-1</sup>	94% (1000)	<sup>112</sup>
MnO <sub>2</sub> nanowire /reduced graphene oxide	1 M Na <sub>2</sub> SO <sub>4</sub>	3 electrode	197.2 F g <sup>-1</sup> at 0.2 A g <sup>-1</sup>	NA	82.2% (10000)	<sup>117</sup>
Fe <sub>2</sub> O <sub>3</sub> on carbon cloth	3 M LiNO <sub>3</sub>	2 electrode symmetric	1565 mF cm <sup>-2</sup> at 1 mA cm <sup>-2</sup>	9.2 mWh cm <sup>-3</sup> , 12 mW cm <sup>-3</sup>	95% (4000)	<sup>120</sup>
Co <sub>3</sub> O <sub>4</sub> carbon composite	2 M KOH	2 electrode symmetric	54 F g <sup>-1</sup> at 0.1 A g <sup>-1</sup>	1.66 W h kg <sup>-1</sup> , 1223 W kg <sup>-1</sup>	82% (10000)	<sup>110</sup>
VO <sub>x</sub> -carbon fiber	LiCl-PVA	2 electrode asymmetric	60.1 F g <sup>-1</sup> at 0.5 mA cm <sup>-2</sup>	0.61 mW h cm <sup>-3</sup> , 0.85 W cm <sup>-3</sup>	87.5% (10000)	<sup>61</sup>
NiO-reduced grapheme oxide	1 M NaOH	2 electrode symmetric	20 F g <sup>-1</sup> at 1 A g <sup>-1</sup>	5.4 W h kg <sup>-1</sup> , 340 W kg <sup>-1</sup>	90% (10000)	<sup>124</sup>

As can be seen from Table 2, the values of specific capacitance, energy, power, and retention are very different due to numerous factors as discussed above. Thus, it may be sometimes difficult to compare the same materials that were used in different configurations and analysis conditions. However, some interesting synthetic results that compare different materials can be proposed.

Figure 11 presents the specific capacitance for different electrode materials by electrode material type. As expected, composite materials the combination of EDLC and pseudocapacitive nature show the highest specific capacitance compared to other groups. Although there is some heterogeneity within each group, the tendency is still relevant.

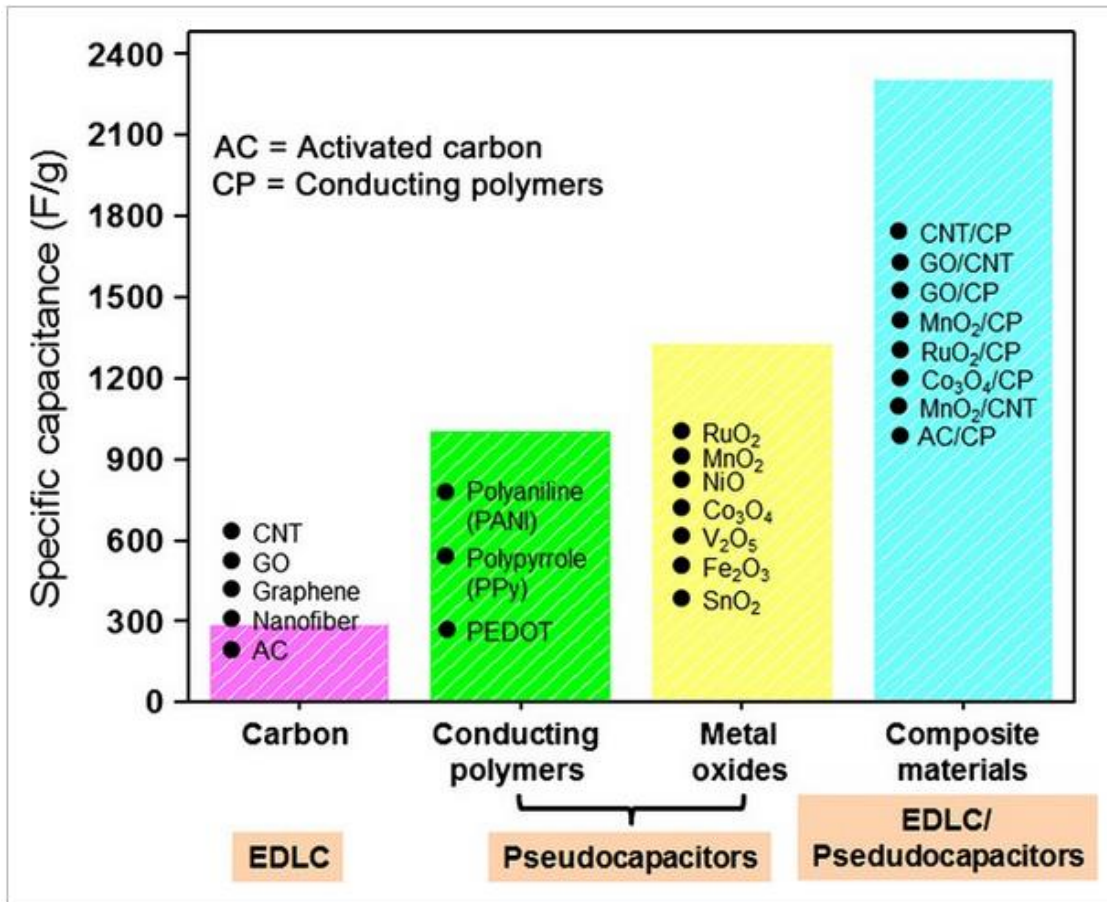


Figure 11 Comparison of specific capacitance for various electrode active materials selected from different categories of supercapacitors: EDLC, pseudocapacitors and EDLC/pseudocapacitors. Figure reprinted from <sup>125</sup>.

### III.3. Carbon/ metal sulfide composites

The quest of finding the appropriate electrode materials remains the most pivotal approach to boosting the energy and power density of supercapacitors and to obtaining their commercialization. As mentioned in the previous part, transition-metal-based materials have been reported through the literature.<sup>126</sup> In particular, transition-metal sulfides (TMS) and their composites gained specific attention due to their high theoretical capacitance, enhanced electric conductivity, and good electrochemical activity compared to their corresponding oxides.<sup>127,128</sup> TMS are semiconductors in the majority of cases, resulting in a better electrical conductivity. The reason comes mainly from the sulfur atom, which has a lower electronegativity than oxygen, which promotes electron transfer and the improvement of electrochemical performance.<sup>129</sup> All of this makes TMS a very potential electrode material. Nevertheless, their huge volume variation and slow kinetic reactions hinder their commercialization and use at a larger scale.

Numerous routes have been proposed to improve the electrochemical performance of TMS. The most used one relies on the synthesis strategies, as it permits controlling the size and shape of the particles. Many synthesis methods were used, such as hydro/solvothermal,<sup>130</sup> coprecipitation<sup>131</sup> and electrodeposition.<sup>132</sup> As for the incorporation of sulfur sources, it includes thioacetamide,<sup>133</sup> thiourea,<sup>134</sup> sodium sulfide<sup>135</sup> and sulfur hydrogen, among others. TMS is a relatively new family of supercapacitor electrode materials compared to that of TMO. However, a tremendous development in tailoring the shape and dimension of the particles is seen.<sup>136</sup> In a similar way to TMO, TMS show the same drawbacks, namely low electronic conductivity, agglomeration and poor cycling stability. One of the most widely used strategies to address this problem is the composite engineering with carbon.<sup>137</sup> Different carbonaceous materials were used as matrix for TMS: graphene oxide<sup>138</sup>, carbon nanotubes (CNT)<sup>139</sup>, nanofibers<sup>140</sup>, etc. Table 3 summarizes the performance of selected TMS/ carbon composites. It can be seen that most of the TMS composites used are employed with alkaline or neutral electrolytes and that the performance is generally determined in three-electrode systems. Thus, one should be aware that these materials would yield a different performance when a symmetric device is used.

*Table 3 : Comparison of carbon/metal sulfide composites as electrode materials for supercapacitors.*

Electrode material	Electrolyte	Type of cell	Specific capacitance	Energy	Power	Refs
CoS <sub>2</sub> -reduced graphite oxide nano fibers	6 M KOH	NA	635.8 F g <sup>-1</sup> at 1 A g <sup>-1</sup>	13.8 W h kg <sup>-1</sup>	824.6 W kg <sup>-1</sup>	140
Co <sub>3</sub> S <sub>4</sub> - reduced graphene oxide	PVA-KOH	Asymmetric	164 F g <sup>-1</sup> at 1 A g <sup>-1</sup>	1.09 W h kg <sup>-1</sup>	398 W kg <sup>-1</sup>	138
CoS-reduced graphene oxide	6 M KOH	Three electrode + symmetric	468 F g <sup>-1</sup> at 1 A g <sup>-1</sup>	30.3 W h kg <sup>-1</sup>	1400 W kg <sup>-1</sup>	141
Co <sub>9</sub> S <sub>8</sub> -3D graphene	1 M KOH	Three electrode + asymmetric	1032.6 F g <sup>-1</sup> at 1 A g <sup>-1</sup>	31.6 W h kg <sup>-1</sup>	910 W kg <sup>-1</sup>	142
MoS <sub>2</sub> -graphene	1 M Na <sub>2</sub> SO <sub>4</sub>	Three electrode + symmetric	210.6 F g <sup>-1</sup> at 1 A g <sup>-1</sup>	10.6 W h kg <sup>-1</sup>	1000 W kg <sup>-1</sup>	143
MoS <sub>2</sub> -3D Graphene network	3 M KOH	Three electrode + asymmetric	2007.8 F g <sup>-1</sup> at 1 A g <sup>-1</sup>	5.59 W h kg <sup>-1</sup>	1281 W kg <sup>-1</sup>	144
Ni <sub>3</sub> S <sub>2</sub> - reduced graphene oxide	2 M KOH	Three electrode	1462 F g <sup>-1</sup> at 1 A g <sup>-1</sup>	NA	NA	145

In a supercapacitor, the electrodes have the same importance as the electrolyte. Therefore, the choice of the two components determines the capacitance, time response, resistivity and hence the energy and power density of the device. The next part highlights the important parameters to consider when choosing an electrolyte, depending on the nature of the latter.

## **IV. Electrolytes**

Electrolytes are an important element of a supercapacitor. According to Eq. 1, the energy density of supercapacitors depends on the capacitance and the square of the cell voltage. Therefore, it would be more efficient to increase the cell voltage than to increase the electrode capacitance in terms of energy density improvement. Hence, developing new electrolytes with a wider potential window should require more attention and effort than developing electrode materials.

The electrolyte is a media that provides the ionic conductivity. Its characteristics (ion type, size, and concentration) directly affect the performance of the supercapacitor. The match between the electrode (pore size) and electrolyte (ion size) determined to ensure good electrochemical behavior (see II.2). Moreover, the supercapacitor cell voltage is strongly limited by the electrochemical stability of the electrolyte within the applied potential.

To date, numerous electrolytes have been reported for energy storage use.<sup>22</sup> Depending on the nature of the electrolyte, they can be classified into two large families: liquid electrolytes and solid electrolytes.<sup>146</sup> Each category can be further divided into small groups as presented in Figure 12. In addition, redox-active electrolytes are also reported.

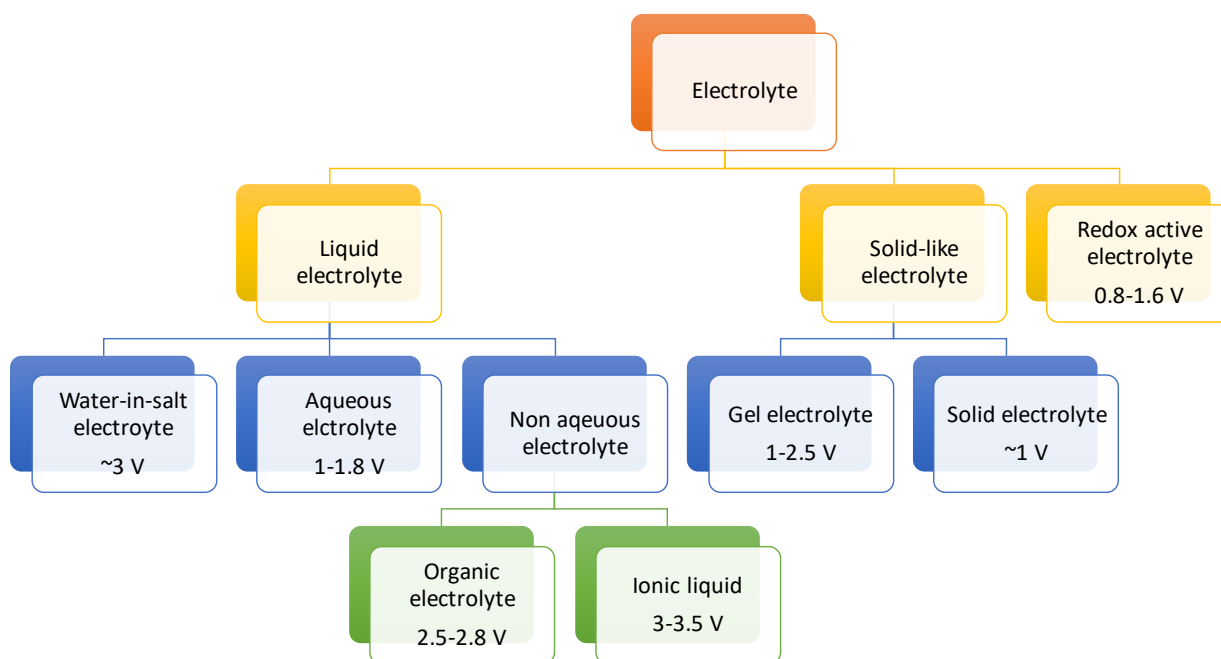


Figure 12 Classification of electrolytes for supercapacitors: liquid, solid-like and redox active along with their specific type of electrolytes.

## IV.1. Liquid electrolytes

Liquid electrolytes are present in the liquid state and are used as solutions in supercapacitors. Their classification can be further divided into three groups depending on the nature of the salt or solvent used: aqueous electrolytes, organic electrolytes, and ionic liquids (IL). They will be discussed in depth in the next section.

### IV.1.1. Aqueous electrolytes

Aqueous electrolytes have high ionic conductivity,<sup>147</sup> low internal resistance but low voltage stability range. Water as a solvent has one of the highest dielectric constant  $\epsilon \approx 80$ , resulting in the highest  $C_s$  values. Thus, aqueous electrolytes are considered to be a convenient and affordable yet limited choice for use in supercapacitors. They operate in a narrower voltage window of 1.23 V, limited by water electrolysis, in comparison to organic electrolytes (2.5-2.8 V) and ionic liquids (3.0-3.5 V), resulting in low energy density (Eq.3). The freezing and the boiling points of the solvent also restraint their temperature range. For all of these reasons, commercial electrolytes (ES) often employ organic electrolytes instead of liquid ones. Nevertheless, aqueous electrolytes are still the most widely used in the research field and the most reported in the literature due to their low cost and easy handling at the laboratory scale. In counterpart, organic electrolytes and ionic liquids require expensive equipment and controlled



atmosphere to avoid moisture. Aqueous electrolytes can be divided according to the pH of the solution into acid electrolytes ( $\text{H}_3\text{PO}_4$ ,  $\text{H}_2\text{SO}_4$ ), neutral electrolytes ( $\text{Na}_2\text{SO}_4$ ,  $\text{K}_2\text{SO}_4$ ) and alkaline electrolytes ( $\text{KOH}$ ,  $\text{LiOH}$ ).

The narrow voltage window of aqueous electrolytes is the main drawback for their larger use, as it limits the energy density that can be derived from a device. Many attempts of extending the voltage window by benefiting from hydrogen sorption at negative sweeps have been suggested.<sup>148</sup> This is mainly developed for neutral electrolytes due to their convenient pH that inhibits water electrolysis.<sup>149</sup> 1 M  $\text{Li}_2\text{SO}_4$  allowed the extension of the voltage window to 1.6 V<sup>150</sup>, while an EC used with  $\text{K}_2\text{SO}_4$  reached 1.9 V.<sup>151</sup>

#### **IV.1.2. Organic electrolytes**

An organic electrolyte is composed of a salt (usually tetraalkylammonium salts, such as tetrafluoroborates or hexafluorophosphates)<sup>152</sup> dissolved in an organic solvent. The latter had high salt solubility and low viscosity. Compared to aqueous electrolytes, organic ones provide a much larger electrochemical window of 2.5 – 2.8 V. This can be directly translated into the improvement of the device energy density. However, their ionic conductivity is lower than that of aqueous ones, they are more expensive because they require purification, and their handling requires special equipment. Due to the lower  $\epsilon$ , the  $C_s$  values of the electrode materials measured in organic solvents are generally lower than those of the aqueous electrolytes. In addition, they commonly use solvents such as acetonitrile (ACN) or propylene carbonate (PC) that are flammable. This results in a potential safety issue on the practical scale.<sup>109</sup>

#### **IV.1.3. Ionic Liquids**

Ionic liquids are salts with fusion points below room temperature that maintain their liquid state and ionic conductivity without the need of a solvent. They have low vapor pressure, high electrochemical operating window 3.0-3.5 V, along with high thermal and electrochemical stability. They are considered the most advantageous electrolytes because of their nonvolatility, nontoxicity, and environmental friendliness. Nevertheless, their high cost and low viscosity impede their utilization in commercial supercapacitors. The most widely used IL is 1-ethyl-3-methylimidazolium tetrafluoroborate (EMIM)( $\text{BF}_4$ ) for its best ionic conductivity among IL.<sup>153</sup>

Table 4 gathers the important characteristics of the three electrolyte families mentioned. It can be seen that each category of liquid electrolytes has its own advantages and drawbacks. For instance, the operating voltage window of IL is promising, but in the counterpart, the high cost

and low viscosity cause are respectively considered inconveniences that need to be handled. In recent years, new ideas have emerged to boost the electrolyte contribution in a supercapacitor. For example, methods such as the introduction of active redox species into the electrolyte were reported and showed a significant increase in the capacitance.<sup>154</sup> Monitoring the pH of the water-based medium was shown to be a crucial aspect in achieving a good electrochemical signature.<sup>155</sup> Regarding the extension of the voltage window, new concentrated electrolytes 'water in salt' proved to be good candidates for this purpose.<sup>156,157</sup>

*Table 4: Different characteristics of aqueous electrolytes divided by categories*

Characteristics	Aqueous electrolytes	Organic electrolytes	Ionic liquids
Ionic conductivity	$>100 \text{ S cm}^{-1}$ <sup>9</sup>	$20 - 60 \text{ S cm}^{-1}$	$<10 \text{ S cm}^{-1}$
Viscosity	$\sim 0.5 \text{ cp}$ <sup>158</sup>	$1 - 12 \text{ cp}$	$41 - 219 \text{ cp}$ <sup>153</sup>
Operating voltage	Alkaline and base $<1 \text{ V}$ Neutral $< 1.8 \text{ V}$	$2.5 - 2.8 \text{ V}$	$3 - 3.5 \text{ V}$
Cost	$<100 \text{ \$ kg}^{-1}$	$345 \text{ \$ kg}^{-1}$	$1328 \text{ \$ kg}^{-1}$

## IV.2. Solid-like electrolytes

A solid-like electrolyte consists of a dry polymer electrolyte or a gel polymer electrolyte. Solid-like electrolytes reduce the risk of leakage, flammability, and corrosion. They are suitable for supercapacitors that can be used in portable, wearable, and bendable electronic devices. In such cases, solid-like electrolytes are of great benefit as they can withstand mechanical stress and are lightweight and eco-friendly.

### IV.2.1. Gel electrolytes

A gel is a solid material composed of two or more components, where one is liquid.<sup>159</sup> Gel electrolytes (GE) are composed of a polymer network and a solvent, where the polymer encapsulates the solvent ions and prevents them from disappearing. In the case of a water solvent, the gel is called a hydrogel.<sup>160</sup> Depending on the nature of the bond, one can distinguish physical or chemical cross-linking between the polymer chains<sup>161</sup>. In physical cross-linking, electrostatic links, hydrogen-bond or chain entanglements connect the chains. While in chemical cross-linking, the type of reactions occurs via covalent bonds.<sup>162</sup> In general, the structure of the host polymer determines the interaction with the solvent and the properties of the resulting gel. The salt consists of free ions and the polymer serves as a conducting medium.

Proton-conducting polymer electrolytes are the most suited for supercapacitor application, due to their high ionic conductivity at room temperature.

Polymers used to develop GE for electrochemical capacitors can be classified according to their origin in natural, synthetic, or natural polymers. Reported synthetic polymers include poly(vinyl) alcohol (PVA)<sup>162</sup>, poly(ethylene oxide) (PEO)<sup>163</sup> and poly(acrylic) acid (PAA)<sup>164</sup>. Among these, PVA has been massively investigated for its excellent chemical stability, good mechanical property, and high water absorbance.<sup>165</sup> The presence of synthetic polymers in electrochemical capacitors does not meet biodegradability and environmental friendliness. That is why some natural polymers have been explored as host for GE in supercapacitors.<sup>162</sup> As natural hosts, we can cite cellulose<sup>166</sup>, agar<sup>167</sup>, chitosan<sup>168</sup> and others.

In the search for low-cost and easy-to-handle devices, various polymers have been used for the preparation of aqueous GE either with acidic<sup>169</sup> or alkaline<sup>170</sup> electrolytes. neutral electrolytes been largely promoted since they extend the potential window of the supercapacitor.<sup>171</sup> Recently, Gajewski *et al.* reported the use of carboxymethylcellulose sodium salt (CMC) impregnated with 1 M Li<sub>2</sub>SO<sub>4</sub> as both hydrogel electrolyte and separator in symmetric carbon supercapacitors.<sup>160</sup> The hydrogel electrolyte allowed improving performance compared to capacitors using commercial separators such as Celgrad or Whatman.

In recent years, different synthesis methodologies have been used to obtain gel electrolytes. The most frequently employed one is the thawing, called the freezing drying technique. Hu *et al.* used this technique on PVA and Kappa-carrageenan (KC) and KOH as an ion source to synthesize the electrolyte PVA / KC / KOH via physical crosslinking.<sup>170</sup> Table 5 presents the electrochemical performance of some GE. Generally, the electrodes used with GE are of carbonaceous nature to benefit from the high SSA and the good stability. When other materials such as the pseudocapacitive one are used, special attention to dissolution problems of the electrode material should be paid. Fabrication of asymmetric capacitors while using a gel electrolyte seems to be an encouraging route to improve the voltage window and the overall metrics of the supercapacitor as is seen in (Table 5).<sup>116</sup>

Table 5 Selected gel electrolytes used for electrochemical capacitors.

Polymer host	Electrolyte	Type of cell	Electrode	Voltage (V)	Capacitance	Energy and power	Refs
(PVA)	Na <sub>2</sub> SO <sub>4</sub> 1 M	Three electrode + symmetric	Microporous activated carbon	1.8	135 F g <sup>-1</sup> at 1 A g <sup>-1</sup>	13 W h kg <sup>-1</sup> at 100 W kg <sup>-1</sup>	<sup>171</sup>
Agar	K <sub>2</sub> SO <sub>4</sub> 0.5 M	Three electrode + symmetric	Activated carbon Kynol 507-20	1.6	100 F g <sup>-1</sup> at 1 A g <sup>-1</sup>	8 W h kg <sup>-1</sup> at 100 W kg <sup>-1</sup>	<sup>167</sup>
Chitosan	EMInBF <sub>4</sub>	2 electrode	Activated carbon	2.5	131 F g <sup>-1</sup> at 2.5 mA cm <sup>-2</sup>	NA	<sup>172</sup>
PVA	6 M KOH	Three electrode + asymmetric	Positive: Co <sub>3</sub> O <sub>4</sub> /carbon composite Negative: Activated carbon	2	235 F g <sup>-1</sup> at 1 A g <sup>-1</sup>	63 W h kg <sup>-1</sup> , 16.2 W kg <sup>-1</sup>	<sup>116</sup>

Although GE have an ionic conductivity one order of magnitude lower than that of liquid electrolytes, their performance withstands conventional capacitors and provides in some cases better metrics. When the manufacturing of the electrode-gel electrolyte interaction is efficient, the performance improves significantly.

#### IV.2.2. Solid electrolytes

Solid electrolytes (SE) are totally solid phase media with significant ionic conductivity. Therefore, no volatility issues are encountered when handling SE electrolytes. On the basis of these criteria, we propose the division of non-liquid electrolytes into gel and solid electrolytes.

Due to their nature, SEs allow the rise of bending, flexible and wearable capacitors used in bendable and portable electronic devices such as smartwatches.<sup>173</sup>

In terms of GE, SE is generally composed of a host, a polymer, and an ion provider. Although they are sometimes described as the same thing as an electrolyte in the literature, we propose a distinction between them. Table 6 presents a brief comparison between gel electrolytes and solid electrolytes. One might remark that the advantages of GE are the drawbacks of SE and vice versa. On one hand, the lower content of water in SE leads to poorer conductivity and performance than GE, but on the other hand it improves the mechanical stability and inhibits the volatility. Therefore, a compromise between water content and mechanical property needs to be achieved.

For SE, the polymer host should have good swelling ability in order to encapsulate as much solvent as possible and increase the water uptake while conserving the solid aspect. Some reports used pore-forming agents such as poly(vinyl pyrrolidone) with PVA, to improve the swelling ratio.<sup>174</sup> In the same study, glutaraldehyde was used as a cross-linking agent to improve the thermal stability of the solid-state electrolyte. This allowed excellent electrochemical performance up to 70 °C compared to the traditional system.

*Table 6 : Comparison between the characteristics of gel electrolytes and solid electrolytes.*

	Advantages	Drawbacks
Gel electrolytes	High content of water Good conductivity Good rate capability	Low stretchability Volatility => Short lifespan Weak cross-linking Strained temperature range
Solid electrolytes	No volatility issues Good tensile stress Good mechanical property Bending angle possible High cross-linking	Low conductivity Lower performance Synthetic polymers => environmental issue Poor electrolyte uptake

Table 7 presents selected SE and their electrochemical performance. Like GE, the most widely used liquid electrolytes for SE are aqueous electrolytes because of their facile handling. Moreover, PVA is the most used host in the literature due to its solubility in water and its excellent mechanical stability.<sup>165</sup> PVA has also been reported to be widely used with KOH, as

this salt softens the polymer chains into an amorphous phase, improving its ionic conductivity.<sup>175</sup>

Table 7 : Selected solid-like electrolytes SE used for electrochemical capacitors.

Polymer host	Electrolyte	Type of cell	Electrode	Voltage window (V)	Capacitance	Energy and power	Refs
PVA	1 M H <sub>2</sub> SO <sub>4</sub>	3 + 2 electrode	Nitrogen doped carbon	1	3.88 F cm <sup>-3</sup> at 0.02 mA cm <sup>-3</sup>	0.09 mWh cm <sup>-3</sup> at 72 mW cm <sup>-3</sup>	<sup>176</sup>
PVA	H <sub>2</sub> SO <sub>4</sub>	symmetric	Graphene	1	187 F g <sup>-1</sup> at 10 mV s <sup>-1</sup>	0.61 W h kg <sup>-1</sup> at 0.67 W kg <sup>-1</sup>	<sup>177</sup>
PVA	LiCl	3 + 2 symmetric electrode	Activated carbon	0.8	297 mF cm <sup>-2</sup> at 0.8 mA cm <sup>-2</sup>	6.6 mW h cm <sup>-2</sup> and 2.4 W cm <sup>-2</sup>	<sup>178</sup>
PVA	2 M H <sub>2</sub> SO <sub>4</sub>	2 symmetric	Graphene-carbon black composite	1	144.5 F g <sup>-1</sup> at 0.5 A g <sup>-1</sup>	NA	<sup>174</sup>
PVA	H <sub>3</sub> PO <sub>4</sub>	2 symmetric	Graphene-polypyrrole	0.8	363 F cm <sup>-3</sup> at 1 mA cm <sup>-3</sup>	NA	<sup>169</sup>

Numerous methods were used to avoid SE drawbacks, i.e. poor conductivity and poor solvent uptake. For example, immersion of electrodes in the corresponding electrolyte solution for 12 h prior to cell assembly was necessary in some cases.<sup>174</sup> In another study, electrode material was immersed in HCl solution for 12h, before being used with the PVA-H<sub>3</sub>PO<sub>4</sub> gel electrolyte.<sup>169</sup>

In addition to mechanical properties amelioration, the chemistry of a polymer can be adjusted in order to provide additional functionalities. For example self-healing, is the case of damaged material, the latter one has the ability to recover its original state.<sup>179</sup> Currently, the process is achieved by introducing reversible crosslinking chemically or physically.

Most SSSs are fabricated on the basis of synthetic polymers, whereas natural polymers are considered to have weak bonds and undergo weak crosslinking. To progress with the need to use bio-sourced and abundant sustainable earth raw materials, the use of natural polymers should be further investigated and improvement of demerits needs to be sought.<sup>180</sup> More recently, a cellulose-based solid state electrolyte has been reported.<sup>181</sup> In addition, cellulose was also used as the electrode precursor. This afforded a flexible, ultra-light, current collector and binder-free supercapacitor (Figure 13). With NaHSO<sub>4</sub> and cellulose as the solid electrolyte, the symmetric device exhibited an operating voltage of 1.5 V, a capacitance of 50 F g<sup>-1</sup> at 0.5 mV s<sup>-1</sup>.<sup>181</sup> This is a step further to build low-cost sustainable supercapacitors, starting from natural renewable and biodegradable materials.

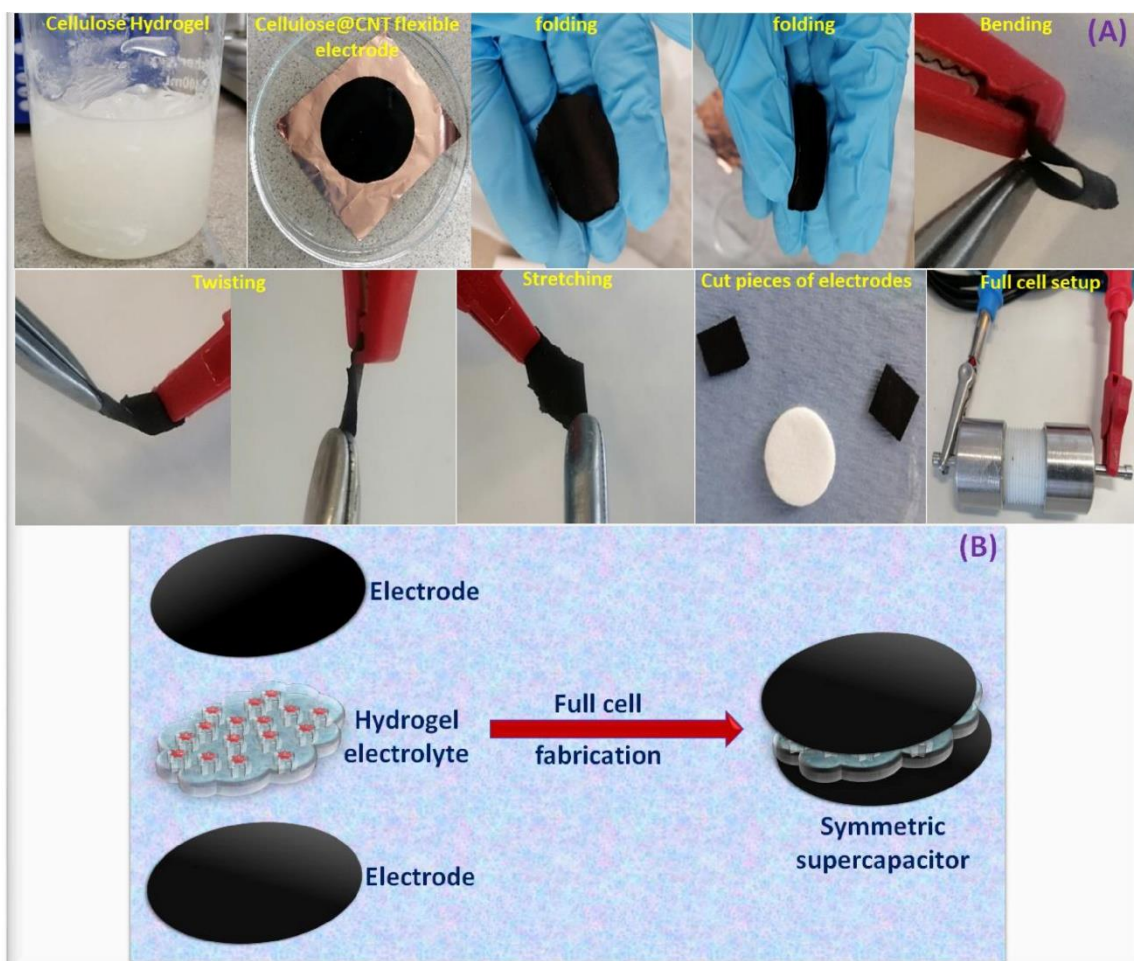


Figure 13: Example of sustainable solid state supercapacitor based on cellulose/NaHSO<sub>4</sub> hydrogel electrolyte. Reprinted from <sup>181</sup> Copyright (2022), with permission from Elsevier.

Overall, solid state supercapacitors are usually used with EDLC materials because of their benefits allowing the obtaining of high energy. Yet, SSS has also been investigated with pseudocapacitive materials, although their low SSA or low conductivity might limit the performance.

SE and GE are beginning to get more attention lately as there has emerged an increased interest in safer and more sustainable energy storage devices. They showed good results, which are in some cases better than the respective liquid electrolytes. For electrode materials, a deep understanding of the kinetics of ions and charge transport within these electrolytes allows us to propose mechanisms for individual systems. Since there are different electrode materials operating with different mechanisms, adequate GE and SE with suitable enough experimental conditions should be ensured.

## **V. Conclusion**

A state of the art of supercapacitors, their operation principles, classifications and key parameters was provided herein. Two main mechanisms of charge storage by electrical double layer and pseudocapacitance were discussed in detail. The description, advantages and limitations were enlisted for both symmetric and asymmetric capacitors. The electrode materials and electrolytes used for such type of device were described. Besides, several important issues such as the different cell types, building procedures, calculation and evaluation methods impacting the performance of different devices were discussed.

The most widely used materials for electrodes, the different synthesis methods, and the design and shape of electrodes are discussed along with their impact on electrochemical performance. Synthesis of carbon materials with different dimensions and internal characteristics (texture, structure, and functionalities) have a direct effect on the performance of the supercapacitor. The introduction of carbon into transition metal oxides and transition metal sulfides is an efficient way to improve the conductivity and limit particle aggregation. The carbon matrix provides a large surface area and facilitates the transport of electrons and ions. Moreover, it permits conservation of the nanoscale effect as it inhibits particle growth that causes poor rate capability. These large various transition metals were used and the different types of their pseudocapacitance were gathered and explained. However, a lack of understanding of the electrochemical storage mechanism hindered further development and improvement of performance. A deeper understanding of the energy storage mechanism of the different metal



oxides/sulfides is required in order to design electrode with maximized performance. Although the characterization of a material by electrochemical techniques in a 3 electrode cell may give promising capacitance, the limitations encountered in real two-electrode devices cause the drastic fall of those values. Therefore, the conditions of the electrochemical measurements should be considered before comparing different materials, and standardized procedures are fully desirable.

A state of the art of current used electrolytes and their classification was also discussed herein. A summarized look at liquid electrolytes was given as they are largely used since decades. As for relatively new emerging electrolytes such as gel and solid electrolytes, the recent advances were provided with an evaluation of the challenges of the different classes of electrolytes. A state of art of employed polymers to date is presented with a critical evaluation of their results. Polyvinyl alcohol is by far the most used host due to its abundance and facile handling. New green natural polymers are emerging and attracted attention lately. To emphasize the sustainable aspect, research is oriented towards sustainable devices containing natural precursors for both electrode and electrolytes.

New characterization tools, such as in situ techniques, are required to be largely spread in order to answer raising questions about new developed capacitors. However, cell construction and experimental conditions may hinder a faithful report of ongoing analysis. Additionally, data interpretation is another aspect that may hamper the true phenomenon of storage mechanisms. However, it is still important to develop and share the current and new results obtained. This brings researchers further to optimizing current systems in order to propose enhanced future energy storage devices.

## References

- (1) Brédas, J.-L.; Buriak, J. M.; Caruso, F.; Choi, K.-S.; Korgel, B. A.; Palacín, M. R.; Persson, K.; Reichmanis, E.; Schüth, F.; Seshadri, R.; Ward, M. D. An Electrifying Choice for the 2019 Chemistry Nobel Prize: Goodenough, Whittingham, and Yoshino. *Chem. Mater.* **2019**, *31* (21), 8577–8581. <https://doi.org/10.1021/acs.chemmater.9b04345>.
- (2) Frackowiak, E.; Abbas, Q.; Béguin, F. Carbon/Carbon Supercapacitors. *Journal of Energy Chemistry* **2013**, *22* (2), 226–240. [https://doi.org/10.1016/S2095-4956\(13\)60028-5](https://doi.org/10.1016/S2095-4956(13)60028-5).
- (3) Noori, A.; El-Kady, M. F.; Rahmanifar, M. S.; Kaner, R. B.; Mousavi, M. F. Towards Establishing Standard Performance Metrics for Batteries, Supercapacitors and Beyond. *Chem. Soc. Rev.* **2019**, *48* (5), 1272–1341. <https://doi.org/10.1039/C8CS00581H>.
- (4) Rand, D. A. J. A Journey on the Electrochemical Road to Sustainability. *J Solid State Electrochem* **2011**, *15* (7), 1579–1622. <https://doi.org/10.1007/s10008-011-1410-z>.
- (5) González, A.; Goikolea, E.; Barrena, J. A.; Mysyk, R. Review on Supercapacitors: Technologies and Materials. *Renewable and Sustainable Energy Reviews* **2016**, *58*, 1189–1206. <https://doi.org/10.1016/j.rser.2015.12.249>.
- (6) Piwek, J.; Platek-Mielczarek, A.; Frackowiak, E.; Fic, K. Enhancing Capacitor Lifetime by Alternate Constant Polarization. *Journal of Power Sources* **2021**, *506*, 230131. <https://doi.org/10.1016/j.jpowsour.2021.230131>.
- (7) Karade, S. S.; Lalwani, S.; Eum, J.-H.; Kim, H. Coin Cell Fabricated Symmetric Supercapacitor Device of Two-Steps Synthesized V2O5 Nanorods. *Journal of Electroanalytical Chemistry* **2020**, *864*, 114080. <https://doi.org/10.1016/j.jelechem.2020.114080>.
- (8) Ojha, M.; Liu, X.; Wu, B.; Deepa, M. Holey Graphitic Carbon Nano-Flakes with Enhanced Storage Characteristics Scaled to a Pouch Cell Supercapacitor. *Fuel* **2021**, *285*, 119246. <https://doi.org/10.1016/j.fuel.2020.119246>.
- (9) Fic, K.; Platek, A.; Piwek, J.; Frackowiak, E. Sustainable Materials for Electrochemical Capacitors. *Materials Today* **2018**, *21* (4), 437–454. <https://doi.org/10.1016/j.mattod.2018.03.005>.
- (10) Ji, H.; Zhao, X.; Qiao, Z.; Jung, J.; Zhu, Y.; Lu, Y.; Zhang, L. L.; MacDonald, A. H.; Ruoff, R. S. Capacitance of Carbon-Based Electrical Double-Layer Capacitors. *Nat Commun* **2014**, *5* (1), 3317. <https://doi.org/10.1038/ncomms4317>.
- (11) Bi, S.; Li, Z.; Xiao, D.; Li, Z.; Mo, T.; Feng, G.; Zhang, X. Pore-Size-Dependent Capacitance and Charging Dynamics of Nanoporous Carbons in Aqueous Electrolytes. *J. Phys. Chem. C* **2022**, *126* (15), 6854–6862. <https://doi.org/10.1021/acs.jpcc.2c01121>.
- (12) Simon, P.; Gogotsi, Y. Perspectives for Electrochemical Capacitors and Related Devices. *Nature Materials* **2020**, *19* (11), 1151–1163. <https://doi.org/10.1038/s41563-020-0747-z>.
- (13) Forse, A. C.; Merlet, C.; Griffin, J. M.; Grey, C. New Perspectives on the Charging Mechanisms of Supercapacitors. *Journal of the American Chemical Society* **2016**, *138* (18), 5731–5744. <https://doi.org/10.1021/jacs.6b02115>.
- (14) Chmiola, J. Anomalous Increase in Carbon Capacitance at Pore Sizes Less Than 1 Nanometer. *Science* **2006**, *313* (5794), 1760–1763. <https://doi.org/10.1126/science.1132195>.
- (15) Largeot, C.; Portet, C.; Chmiola, J.; Taberna, P.-L.; Gogotsi, Y.; Simon, P. Relation between the Ion Size and Pore Size for an Electric Double-Layer Capacitor. *J. Am. Chem. Soc.* **2008**, *130* (9), 2730–2731. <https://doi.org/10.1021/ja7106178>.
- (16) Jiang, D.; Jin, Z.; Henderson, D.; Wu, J. Solvent Effect on the Pore-Size Dependence of an Organic Electrolyte Supercapacitor. *J. Phys. Chem. Lett.* **2012**, *3* (13), 1727–1731. <https://doi.org/10.1021/jz3004624>.
- (17) Yan, J.; Wang, Q.; Wei, T.; Jiang, L.; Zhang, M.; Jing, X.; Fan, Z. Template-Assisted Low Temperature Synthesis of Functionalized Graphene for Ultrahigh Volumetric Performance Supercapacitors. *ACS Nano* **2014**, *8* (5), 4720–4729. <https://doi.org/10.1021/nn500497k>.
- (18) Ba, H.; Wang, W.; Tuci, G.; Pronkin, S. N.; Weinberg, C.; Nguyen-Dinh, L.; Giambastiani, G.; Pham-Huu, C. Tridimensional Few-Layer Graphene-like Structures from Sugar-Salt Mixtures as

- High-Performance Supercapacitor Electrodes. *Materials Today Energy* **2018**, *10*, 118–125. <https://doi.org/10.1016/j.mtener.2018.08.015>.
- (19) A. Centeno, T.; Sereda, O.; Stoeckli, F. Capacitance in Carbon Pores of 0.7 to 15 Nm: A Regular Pattern. *Physical Chemistry Chemical Physics* **2011**, *13* (27), 12403–12406. <https://doi.org/10.1039/C1CP20748B>.
- (20) Platek-Mielczarek, A.; Nita, C.; Matei Ghimbeu, C.; Frackowiak, E.; Fic, K. Link between Alkali Metals in Salt Templates and in Electrolytes for Improved Carbon-Based Electrochemical Capacitors. *ACS Appl. Mater. Interfaces* **2021**, *13* (2), 2584–2599. <https://doi.org/10.1021/acsami.0c18627>.
- (21) Ruch, P. W.; Cericola, D.; Foelske, A.; Kötz, R.; Wokaun, A. A Comparison of the Aging of Electrochemical Double Layer Capacitors with Acetonitrile and Propylene Carbonate-Based Electrolytes at Elevated Voltages. *Electrochimica Acta* **2010**, *55* (7), 2352–2357. <https://doi.org/10.1016/j.electacta.2009.11.098>.
- (22) Béguin, F.; Presser, V.; Balducci, A.; Frackowiak, E. Carbons and Electrolytes for Advanced Supercapacitors. *Advanced Materials* **2014**, *26* (14), 2219–2251. <https://doi.org/10.1002/adma.201304137>.
- (23) Castro-Gutiérrez, J.; Díez, N.; Sevilla, M.; Izquierdo, M. T.; Celzard, A.; Fierro, V. Model Carbon Materials Derived from Tannin to Assess the Importance of Pore Connectivity in Supercapacitors. *Renewable and Sustainable Energy Reviews* **2021**, *151*, 111600. <https://doi.org/10.1016/j.rser.2021.111600>.
- (24) Brousse, T.; Bélanger, D.; Long, J. W. To Be or Not To Be Pseudocapacitive? *J. Electrochem. Soc.* **2015**, *162* (5), A5185–A5189. <https://doi.org/10.1149/2.0201505jes>.
- (25) Augustyn, V.; Simon, P.; Dunn, B. Pseudocapacitive Oxide Materials for High-Rate Electrochemical Energy Storage. *Energy & Environmental Science* **2014**, *7* (5), 1597–1614. <https://doi.org/10.1039/C3EE44164D>.
- (26) Fleischmann, S.; Mitchell, J. B.; Wang, R.; Zhan, C.; Jiang, D.; Presser, V.; Augustyn, V. Pseudocapacitance: From Fundamental Understanding to High Power Energy Storage Materials. *Chem. Rev.* **2020**, *120* (14), 6738–6782. <https://doi.org/10.1021/acs.chemrev.0c00170>.
- (27) Trasatti, S.; Buzzanca, G. Ruthenium Dioxide: A New Interesting Electrode Material. Solid State Structure and Electrochemical Behaviour. *Journal of Electroanalytical Chemistry and Interfacial Electrochemistry* **1971**, *29* (2), A1–A5. [https://doi.org/10.1016/S0022-0728\(71\)80111-0](https://doi.org/10.1016/S0022-0728(71)80111-0).
- (28) Ardizzone, S.; Fregonara, G.; Trasatti, S. “Inner” and “Outer” Active Surface of RuO<sub>2</sub> Electrodes. *Electrochimica Acta* **1990**, *35* (1), 263–267. [https://doi.org/10.1016/0013-4686\(90\)85068-X](https://doi.org/10.1016/0013-4686(90)85068-X).
- (29) Long, J. W.; Swider, K. E.; Merzbacher, C. I.; Rolison, D. R. Voltammetric Characterization of Ruthenium Oxide-Based Aerogels and Other RuO<sub>2</sub> Solids: The Nature of Capacitance in Nanostructured Materials. *Langmuir* **1999**, *15* (3), 780–785. <https://doi.org/10.1021/la980785a>.
- (30) Lee, H. Y.; Goodenough, J. B. Supercapacitor Behavior with KCl Electrolyte. *Journal of Solid State Chemistry* **1999**, *144* (1), 220–223. <https://doi.org/10.1006/jssc.1998.8128>.
- (31) Conway, B. E. *Electrochemical Supercapacitors: Scientific Fundamentals and Technological Applications*; Springer Science & Business Media, 2013.
- (32) Gogotsi, Y.; Simon, P. True Performance Metrics in Electrochemical Energy Storage. *Science* **2011**, *334* (6058), 917–918. <https://doi.org/10.1126/science.1213003>.
- (33) Come, J.; Augustyn, V.; Kim, J. W.; Rozier, P.; Taberna, P.-L.; Gogotsi, P.; Long, J. W.; Dunn, B.; Simon, P. Electrochemical Kinetics of Nanostructured Nb<sub>2</sub>O<sub>5</sub> Electrodes. *J. Electrochem. Soc.* **2014**, *161* (5), A718. <https://doi.org/10.1149/2.040405jes>.
- (34) Dong, W.; Rolison, D. R.; Dunna, B. Electrochemical Properties of High Surface Area Vanadium Oxide Aerogels. *Electrochem. Solid-State Lett.* **2000**, *3* (10), 457. <https://doi.org/10.1149/1.1391178>.
- (35) Naoi, K.; Kurita, T.; Abe, M.; Furuhashi, T.; Abe, Y.; Okazaki, K.; Miyamoto, J.; Iwama, E.; Aoyagi, S.; Naoi, W.; Simon, P. Ultrafast Nanocrystalline-TiO<sub>2</sub>(B)/Carbon Nanotube Hyperdispersion Prepared via Combined Ultracentrifugation and Hydrothermal Treatments for Hybrid

- Supercapacitors. *Advanced Materials* **2016**, *28* (31), 6751–6757. <https://doi.org/10.1002/adma.201600798>.
- (36) Okubo, M.; Hosono, E.; Kim, J.; Enomoto, M.; Kojima, N.; Kudo, T.; Zhou, H.; Honma, I. Nanosize Effect on High-Rate Li-Ion Intercalation in LiCoO<sub>2</sub> Electrode. *J. Am. Chem. Soc.* **2007**, *129* (23), 7444–7452. <https://doi.org/10.1021/ja0681927>.
- (37) Costentin, C.; Porter, T. R.; Savéant, J.-M. How Do Pseudocapacitors Store Energy? Theoretical Analysis and Experimental Illustration. *ACS Appl. Mater. Interfaces* **2017**, *9* (10), 8649–8658. <https://doi.org/10.1021/acsami.6b14100>.
- (38) *An approach to classification and capacitance expressions in electrochemical capacitors technology - Physical Chemistry Chemical Physics (RSC Publishing)* DOI:10.1039/C4CP05124F. <https://pubs.rsc.org/en/content/articlehtml/2015/cp/c4cp05124f> (accessed 2020-09-28).
- (39) Dong, Y.; Zhu, J.; Li, Q.; Zhang, S.; Song, H.; Jia, D. Carbon Materials for High Mass-Loading Supercapacitors: Filling the Gap between New Materials and Practical Applications. *Journal of Materials Chemistry A* **2020**, *8* (42), 21930–21946. <https://doi.org/10.1039/D0TA08265A>.
- (40) Abouali, S.; Akbari Garakani, M.; Zhang, B.; Xu, Z.-L.; Kamali Heidari, E.; Huang, J.; Huang, J.; Kim, J.-K. Electrospun Carbon Nanofibers with in Situ Encapsulated Co<sub>3</sub>O<sub>4</sub> Nanoparticles as Electrodes for High-Performance Supercapacitors. *ACS Appl. Mater. Interfaces* **2015**, *7* (24), 13503–13511. <https://doi.org/10.1021/acsami.5b02787>.
- (41) Noked, M.; Soffer, A.; Aurbach, D. The Electrochemistry of Activated Carbonaceous Materials: Past, Present, and Future. *J Solid State Electrochem* **2011**, *15* (7), 1563. <https://doi.org/10.1007/s10008-011-1411-y>.
- (42) Trogadas, P.; Fuller, T. F.; Strasser, P. Carbon as Catalyst and Support for Electrochemical Energy Conversion. *Carbon* **2014**, *75*, 5–42. <https://doi.org/10.1016/j.carbon.2014.04.005>.
- (43) Frumkin, A. N.; Petrii, O. A. Potentials of Zero Total and Zero Free Charge of Platinum Group Metals. *Electrochimica Acta* **1975**, *20* (5), 347–359. [https://doi.org/10.1016/0013-4686\(75\)90017-1](https://doi.org/10.1016/0013-4686(75)90017-1).
- (44) Golub, D.; Soffer, A.; Oren, Y. The Electrical Double Layer of Carbon and Graphite Electrodes: Part V. Specific Interactions with Simple Ions. *Journal of Electroanalytical Chemistry and Interfacial Electrochemistry* **1989**, *260* (2), 383–392. [https://doi.org/10.1016/0022-0728\(89\)87152-9](https://doi.org/10.1016/0022-0728(89)87152-9).
- (45) Shao, L.-H.; Biener, J.; Kramer, D.; N. Viswanath, R.; F. Baumann, T.; V. Hamza, A.; Weissmüller, J. Electrocapillary Maximum and Potential of Zero Charge of Carbon Aerogel. *Physical Chemistry Chemical Physics* **2010**, *12* (27), 7580–7587. <https://doi.org/10.1039/B916331J>.
- (46) Wu, T.; Wang, G.; Zhan, F.; Dong, Q.; Ren, Q.; Wang, J.; Qiu, J. Surface-Treated Carbon Electrodes with Modified Potential of Zero Charge for Capacitive Deionization. *Water Research* **2016**, *93*, 30–37. <https://doi.org/10.1016/j.watres.2016.02.004>.
- (47) Stoller, M. D.; Ruoff, R. S. Best Practice Methods for Determining an Electrode Material's Performance for Ultracapacitors. *Energy Environ. Sci.* **2010**, *3* (9), 1294. <https://doi.org/10.1039/c0ee00074d>.
- (48) Mathis, T. S.; Kurra, N.; Wang, X.; Pinto, D.; Simon, P.; Gogotsi, Y. Energy Storage Data Reporting in Perspective—Guidelines for Interpreting the Performance of Electrochemical Energy Storage Systems. *Adv. Energy Mater.* **2019**, *9* (39), 1902007. <https://doi.org/10.1002/aenm.201902007>.
- (49) Xie, J.; Yang, P.; Wang, Y.; Qi, T.; Lei, Y.; Li, C. M. Puzzles and Confusions in Supercapacitor and Battery: Theory and Solutions. *Journal of Power Sources* **2018**, *401*, 213–223. <https://doi.org/10.1016/j.jpowsour.2018.08.090>.
- (50) Choudhary, N.; Li, C.; Moore, J.; Nagaiah, N.; Zhai, L.; Jung, Y.; Thomas, J. Asymmetric Supercapacitor Electrodes and Devices. *Advanced Materials* **2017**, *29* (21), 1605336. <https://doi.org/10.1002/adma.201605336>.
- (51) Shao, Y.; El-Kady, M. F.; Sun, J.; Li, Y.; Zhang, Q.; Zhu, M.; Wang, H.; Dunn, B.; Kaner, R. B. Design and Mechanisms of Asymmetric Supercapacitors. *Chem. Rev.* **2018**, *118* (18), 9233–9280. <https://doi.org/10.1021/acs.chemrev.8b00252>.

- (52) Wang, F.; Xiao, S.; Hou, Y.; Hu, C.; Liu, L.; Wu, Y. Electrode Materials for Aqueous Asymmetric Supercapacitors. *RSC Advances* **2013**, *3* (32), 13059–13084. <https://doi.org/10.1039/C3RA23466E>.
- (53) Peng, H.; Ma, G.; Sun, K.; Mu, J.; Luo, M.; Lei, Z. High-Performance Aqueous Asymmetric Supercapacitor Based on Carbon Nanofibers Network and Tungsten Trioxide Nanorod Bundles Electrodes. *Electrochimica Acta* **2014**, *147*, 54–61. <https://doi.org/10.1016/j.electacta.2014.09.100>.
- (54) P. Dubal, D.; R. Chodankar, N.; Kim, D.-H.; Gomez-Romero, P. Towards Flexible Solid-State Supercapacitors for Smart and Wearable Electronics. *Chemical Society Reviews* **2018**, *47* (6), 2065–2129. <https://doi.org/10.1039/C7CS00505A>.
- (55) Khomenko, V.; Raymundo-Piñero, E.; Béguin, F. Optimisation of an Asymmetric Manganese Oxide/Activated Carbon Capacitor Working at 2V in Aqueous Medium. *Journal of Power Sources* **2006**, *153* (1), 183–190. <https://doi.org/10.1016/j.jpowsour.2005.03.210>.
- (56) Su, F.; Miao, M. Asymmetric Carbon Nanotube–MnO<sub>2</sub>/Carbon Nanotube–MnO<sub>2</sub> Two-Ply Yarn Supercapacitors for Wearable Electronics. *Nanotechnology* **2014**, *25* (13), 135401. <https://doi.org/10.1088/0957-4484/25/13/135401>.
- (57) Gill Choi, B.; Chang, S.-J.; Kang, H.-W.; Pil Park, C.; Jin Kim, H.; Hi Hong, W.; Lee, S.; Suk Huh, Y. High Performance of a Solid-State Flexible Asymmetric Supercapacitor Based on Graphene Films. *Nanoscale* **2012**, *4* (16), 4983–4988. <https://doi.org/10.1039/C2NR30991B>.
- (58) Hwang, J. Y.; El-Kady, M. F.; Wang, Y.; Wang, L.; Shao, Y.; Marsh, K.; Ko, J. M.; Kaner, R. B. Direct Preparation and Processing of Graphene/RuO<sub>2</sub> Nanocomposite Electrodes for High-Performance Capacitive Energy Storage. *Nano Energy* **2015**, *18*, 57–70. <https://doi.org/10.1016/j.nanoen.2015.09.009>.
- (59) Yang, P.; Ding, Y.; Lin, Z.; Chen, Z.; Li, Y.; Qiang, P.; Ebrahimi, M.; Mai, W.; Wong, C. P.; Wang, Z. L. Low-Cost High-Performance Solid-State Asymmetric Supercapacitors Based on MnO<sub>2</sub> Nanowires and Fe<sub>2</sub>O<sub>3</sub> Nanotubes. *Nano Lett.* **2014**, *14* (2), 731–736. <https://doi.org/10.1021/nl404008e>.
- (60) Zhu, J.; Huang, L.; Xiao, Y.; Shen, L.; Chen, Q.; Shi, W. Hydrogenated CoO x Nanowire@Ni(OH)<sub>2</sub> Nanosheet Core–Shell Nanostructures for High-Performance Asymmetric Supercapacitors. *Nanoscale* **2014**, *6* (12), 6772–6781. <https://doi.org/10.1039/C4NR00771A>.
- (61) Lu, X.; Yu, M.; Zhai, T.; Wang, G.; Xie, S.; Liu, T.; Liang, C.; Tong, Y.; Li, Y. High Energy Density Asymmetric Quasi-Solid-State Supercapacitor Based on Porous Vanadium Nitride Nanowire Anode. *Nano Lett.* **2013**, *13* (6), 2628–2633. <https://doi.org/10.1021/nl400760a>.
- (62) Jiang, H.; Li, C.; Sun, T.; Ma, J. A Green and High Energy Density Asymmetric Supercapacitor Based on Ultrathin MnO<sub>2</sub> Nanostructures and Functional Mesoporous Carbon Nanotube Electrodes. *Nanoscale* **2012**, *4* (3), 807–812. <https://doi.org/10.1039/C1NR11542A>.
- (63) Wu, N.; Bai, X.; Pan, D.; Dong, B.; Wei, R.; Naik, N.; Patil, R. R.; Guo, Z. Recent Advances of Asymmetric Supercapacitors. *Advanced Materials Interfaces* **2021**, *8* (1), 2001710. <https://doi.org/10.1002/admi.202001710>.
- (64) Huang, S.; Zhu, X.; Sarkar, S.; Zhao, Y. Challenges and Opportunities for Supercapacitors. *APL Materials* **2019**, *7* (10), 100901. <https://doi.org/10.1063/1.5116146>.
- (65) Dutch, S. I. Periodic Tables of Elemental Abundance. *J. Chem. Educ.* **1999**, *76* (3), 356. <https://doi.org/10.1021/ed076p356>.
- (66) Serp, P.; Figueiredo, J. L. *Carbon Materials for Catalysis*; John Wiley & Sons, 2009.
- (67) Sánchez-González, J.; Macías-García, A.; Alexandre-Franco, M. F.; Gómez-Serrano, V. Electrical Conductivity of Carbon Blacks under Compression. *Carbon* **2005**, *43* (4), 741–747. <https://doi.org/10.1016/j.carbon.2004.10.045>.
- (68) Barroso Bogeat, A. Understanding and Tuning the Electrical Conductivity of Activated Carbon: A State-of-the-Art Review. *Critical Reviews in Solid State and Materials Sciences* **2021**, *46* (1), 1–37. <https://doi.org/10.1080/10408436.2019.1671800>.

- (69) Li, H.; Kang, Z.; Liu, Y.; Lee, S.-T. Carbon Nanodots: Synthesis, Properties and Applications. *Journal of Materials Chemistry* **2012**, *22* (46), 24230–24253. <https://doi.org/10.1039/C2JM34690G>.
- (70) Zhang, B.; Liu, C.; Liu, Y. A Novel One-Step Approach to Synthesize Fluorescent Carbon Nanoparticles. *European Journal of Inorganic Chemistry* **2010**, *2010* (28), 4411–4414. <https://doi.org/10.1002/ejic.201000622>.
- (71) Gutiérrez-Sánchez, C.; Mediavilla, M.; Guerrero-Esteban, T.; Revenga-Parra, M.; Pariente, F.; Lorenzo, E. Direct Covalent Immobilization of New Nitrogen-Doped Carbon Nanodots by Electrografting for Sensing Applications. *Carbon* **2020**, *159*, 303–310. <https://doi.org/10.1016/j.carbon.2019.12.053>.
- (72) Strauss, V.; Marsh, K.; Kowal, M. D.; El-Kady, M.; Kaner, R. B. A Simple Route to Porous Graphene from Carbon Nanodots for Supercapacitor Applications. *Advanced Materials* **2018**, *30* (8), 1704449. <https://doi.org/10.1002/adma.201704449>.
- (73) Kumar, V. B.; Borenstein, A.; Markovsky, B.; Aurbach, D.; Gedanken, A.; Talianker, M.; Porat, Z. Activated Carbon Modified with Carbon Nanodots as Novel Electrode Material for Supercapacitors. *J. Phys. Chem. C* **2016**, *120* (25), 13406–13413. <https://doi.org/10.1021/acs.jpcc.6b04045>.
- (74) Wang, C.; Strauss, V.; Kaner, R. B. Carbon Nanodots for Capacitor Electrodes. *Trends in Chemistry* **2019**, *1* (9), 858–868. <https://doi.org/10.1016/j.trechm.2019.05.009>.
- (75) Zhang, S.; Zhu, J.; Qing, Y.; Wang, L.; Zhao, J.; Li, J.; Tian, W.; Jia, D.; Fan, Z. Ultramicroporous Carbons Puzzled by Graphene Quantum Dots: Integrated High Gravimetric, Volumetric, and Areal Capacitances for Supercapacitors. *Advanced Functional Materials* **2018**, *28* (52), 1805898. <https://doi.org/10.1002/adfm.201805898>.
- (76) Hu, Y.; Quan, H.; Cui, J.; Luo, W.; Zeng, W.; Chen, D. Carbon Nanodot Modified N, O-Doped Porous Carbon for Solid-State Supercapacitor: A Comparative Study with Carbon Nanotube and Graphene Oxide. *Journal of Alloys and Compounds* **2021**, *877*, 160237. <https://doi.org/10.1016/j.jallcom.2021.160237>.
- (77) Pandolfo, A. G.; Hollenkamp, A. F. Carbon Properties and Their Role in Supercapacitors. *Journal of Power Sources* **2006**, *157* (1), 11–27. <https://doi.org/10.1016/j.jpowsour.2006.02.065>.
- (78) Strauss, V.; Anderson, M.; Wang, C.; Borenstein, A.; Kaner, R. B. Carbon Nanodots as Feedstock for a Uniform Hematite-Graphene Nanocomposite. *Small* **2018**, *14* (51), 1803656. <https://doi.org/10.1002/sml.201803656>.
- (79) Oloore, L. E.; Gondal, M. A.; Popoola, A.; Popoola, I. K. Surface Capacitive Charge Storage in Carbon Nanodots-Anchored Hybrid Halide Perovskites. *Carbon* **2021**, *173*, 1048–1058. <https://doi.org/10.1016/j.carbon.2020.11.097>.
- (80) Portet, C.; Yushin, G.; Gogotsi, Y. Electrochemical Performance of Carbon Onions, Nanodiamonds, Carbon Black and Multiwalled Nanotubes in Electrical Double Layer Capacitors. *Carbon* **2007**, *45* (13), 2511–2518. <https://doi.org/10.1016/j.carbon.2007.08.024>.
- (81) McDonough, J. K.; Frolov, A. I.; Presser, V.; Niu, J.; Miller, C. H.; Ubieto, T.; Fedorov, M. V.; Gogotsi, Y. Influence of the Structure of Carbon Onions on Their Electrochemical Performance in Supercapacitor Electrodes. *Carbon* **2012**, *50* (9), 3298–3309. <https://doi.org/10.1016/j.carbon.2011.12.022>.
- (82) Pech, D.; Brunet, M.; Durou, H.; Huang, P.; Mochalin, V.; Gogotsi, Y.; Taberna, P.-L.; Simon, P. Ultrahigh-Power Micrometre-Sized Supercapacitors Based on Onion-like Carbon. *Nature Nanotech* **2010**, *5* (9), 651–654. <https://doi.org/10.1038/nnano.2010.162>.
- (83) Moussa, G.; Matei Ghimbeu, C.; Taberna, P.-L.; Simon, P.; Vix-Guterl, C. Relationship between the Carbon Nano-Onions (CNOs) Surface Chemistry/Defects and Their Capacitance in Aqueous and Organic Electrolytes. *Carbon* **2016**, *105*, 628–637. <https://doi.org/10.1016/j.carbon.2016.05.010>.
- (84) Li Zhang, L.; S. Zhao, X. Carbon-Based Materials as Supercapacitor Electrodes. *Chemical Society Reviews* **2009**, *38* (9), 2520–2531. <https://doi.org/10.1039/B813846J>.

- (85) Pan, H.; Li, J.; Feng, Y. Carbon Nanotubes for Supercapacitor. *Nanoscale Res Lett* **2010**, *5* (3), 654–668. <https://doi.org/10.1007/s11671-009-9508-2>.
- (86) Zhu, Y.; Murali, S.; Cai, W.; Li, X.; Suk, J. W.; Potts, J. R.; Ruoff, R. S. Graphene and Graphene Oxide: Synthesis, Properties, and Applications. *Advanced Materials* **2010**, *22* (35), 3906–3924. <https://doi.org/10.1002/adma.201001068>.
- (87) Chen, K.; Song, S.; Liu, F.; Xue, D. Structural Design of Graphene for Use in Electrochemical Energy Storage Devices. *Chemical Society Reviews* **2015**, *44* (17), 6230–6257. <https://doi.org/10.1039/C5CS00147A>.
- (88) Pei, S.; Cheng, H.-M. The Reduction of Graphene Oxide. *Carbon* **2012**, *50* (9), 3210–3228. <https://doi.org/10.1016/j.carbon.2011.11.010>.
- (89) Wang, Y.; Wu, Y.; Huang, Y.; Zhang, F.; Yang, X.; Ma, Y.; Chen, Y. Preventing Graphene Sheets from Restacking for High-Capacitance Performance. *J. Phys. Chem. C* **2011**, *115* (46), 23192–23197. <https://doi.org/10.1021/jp206444e>.
- (90) Hummers, W. S.; Offeman, R. E. Preparation of Graphitic Oxide. *J. Am. Chem. Soc.* **1958**, *80* (6), 1339–1339. <https://doi.org/10.1021/ja01539a017>.
- (91) Marcano, D. C.; Kosynkin, D. V.; Berlin, J. M.; Sinitskii, A.; Sun, Z.; Slesarev, A.; Alemany, L. B.; Lu, W.; Tour, J. M. Improved Synthesis of Graphene Oxide. *ACS Nano* **2010**, *4* (8), 4806–4814. <https://doi.org/10.1021/nn1006368>.
- (92) Ciesielski, A.; Samorì, P. Graphene via Sonication Assisted Liquid-Phase Exfoliation. *Chemical Society Reviews* **2014**, *43* (1), 381–398. <https://doi.org/10.1039/C3CS60217F>.
- (93) Ihiawakrim, D.; Ersen, O.; Melin, F.; Hellwig, P.; Janowska, I.; Begin, D.; Baaziz, W.; Begin-Colin, S.; Pham-Huu, C.; Baati, R. A Single-Stage Functionalization and Exfoliation Method for the Production of Graphene in Water : Stepwise Construction of 2D-Nanostructured Composites with Iron Oxide Nanoparticles. *Nanoscale* **2013**, *5* (19), 9073–9080. <https://doi.org/10.1039/C3NR02684A>.
- (94) Hamze, S.; Berrada, N.; Cabaleiro, D.; Desforges, A.; Ghanbaja, J.; Gleize, J.; Bégin, D.; Michaux, F.; Maré, T.; Vigolo, B.; Estellé, P. Few-Layer Graphene-Based Nanofluids with Enhanced Thermal Conductivity. *Nanomaterials* **2020**, *10* (7), 1258. <https://doi.org/10.3390/nano10071258>.
- (95) Li, D.; Kaner, R. B. Graphene-Based Materials. *Science* **2008**, *320* (5880), 1170–1171. <https://doi.org/10.1126/science.1158180>.
- (96) Ke, Q.; Wang, J. Graphene-Based Materials for Supercapacitor Electrodes – A Review. *Journal of Materiomics* **2016**, *2* (1), 37–54. <https://doi.org/10.1016/j.jmat.2016.01.001>.
- (97) Xia, Z. Y.; Pezzini, S.; Treossi, E.; Giambastiani, G.; Corticelli, F.; Morandi, V.; Zanelli, A.; Bellani, V.; Palermo, V. The Exfoliation of Graphene in Liquids by Electrochemical, Chemical, and Sonication-Assisted Techniques: A Nanoscale Study. *Advanced Functional Materials* **2013**, *23* (37), 4684–4693. <https://doi.org/10.1002/adfm.201203686>.
- (98) Fan, Z.; Yan, J.; Zhi, L.; Zhang, Q.; Wei, T.; Feng, J.; Zhang, M.; Qian, W.; Wei, F. A Three-Dimensional Carbon Nanotube/Graphene Sandwich and Its Application as Electrode in Supercapacitors. *Advanced Materials* **2010**, *22* (33), 3723–3728. <https://doi.org/10.1002/adma.201001029>.
- (99) Cheng, Q.; Tang, J.; Ma, J.; Zhang, H.; Shinya, N.; Qin, L.-C. Graphene and Carbon Nanotube Composite Electrodes for Supercapacitors with Ultra-High Energy Density. *Physical Chemistry Chemical Physics* **2011**, *13* (39), 17615–17624. <https://doi.org/10.1039/C1CP21910C>.
- (100) Wang, H.; Sun, X.; Liu, Z.; Lei, Z. Creation of Nanopores on Graphene Planes with MgO Template for Preparing High-Performance Supercapacitor Electrodes. *Nanoscale* **2014**, *6* (12), 6577–6584. <https://doi.org/10.1039/C4NR00538D>.
- (101) Wei, L.; Yushin, G. Nanostructured Activated Carbons from Natural Precursors for Electrical Double Layer Capacitors. *Nano Energy* **2012**, *1* (4), 552–565. <https://doi.org/10.1016/j.nanoen.2012.05.002>.
- (102) Yoo, S.; Kelley, S. S.; Tilotta, D. C.; Park, S. Structural Characterization of Loblolly Pine Derived Biochar by X-Ray Diffraction and Electron Energy Loss Spectroscopy. *ACS Sustainable Chem. Eng.* **2018**, *6* (2), 2621–2629. <https://doi.org/10.1021/acssuschemeng.7b04119>.

- (103) Senthil, C.; Lee, C. W. Biomass-Derived Biochar Materials as Sustainable Energy Sources for Electrochemical Energy Storage Devices. *Renewable and Sustainable Energy Reviews* **2021**, *137*, 110464. <https://doi.org/10.1016/j.rser.2020.110464>.
- (104) Ukanwa, K. S.; Patchigolla, K.; Sakrabani, R.; Anthony, E.; Mandavgane, S. A Review of Chemicals to Produce Activated Carbon from Agricultural Waste Biomass. *Sustainability* **2019**, *11* (22), 6204. <https://doi.org/10.3390/su11226204>.
- (105) Zhi, M.; Xiang, C.; Li, J.; Li, M.; Wu, N. Nanostructured Carbon–Metal Oxide Composite Electrodes for Supercapacitors: A Review. *Nanoscale* **2013**, *5* (1), 72–88. <https://doi.org/10.1039/C2NR32040A>.
- (106) Wang, T.; Chen, H. C.; Yu, F.; Zhao, X. S.; Wang, H. Boosting the Cycling Stability of Transition Metal Compounds–Based Supercapacitors. *Energy Storage Materials* **2019**, *16*, 545–573. <https://doi.org/10.1016/j.ensm.2018.09.007>.
- (107) Liang, K.; Tang, X.; Hu, W. High-Performance Three-Dimensional Nanoporous NiO Film as a Supercapacitor Electrode. *Journal of Materials Chemistry* **2012**, *22* (22), 11062–11067. <https://doi.org/10.1039/C2JM31526B>.
- (108) Mohd Abdah, M. A. A.; Azman, N. H. N.; Kulandaivalu, S.; Sulaiman, Y. Review of the Use of Transition-Metal-Oxide and Conducting Polymer-Based Fibres for High-Performance Supercapacitors. *Materials & Design* **2020**, *186*, 108199. <https://doi.org/10.1016/j.matdes.2019.108199>.
- (109) An, C.; Zhang, Y.; Guo, H.; Wang, Y. Metal Oxide-Based Supercapacitors: Progress and Prospectives. *Nanoscale Adv.* **2019**, *1* (12), 4644–4658. <https://doi.org/10.1039/C9NA00543A>.
- (110) Zallouz, S.; Réty, B.; Vidal, L.; Le Meins, J.-M.; Matei Ghimbeu, C. Co<sub>3</sub>O<sub>4</sub> Nanoparticles Embedded in Mesoporous Carbon for Supercapacitor Applications. *ACS Appl. Nano Mater.* **2021**, *4* (5), 5022–5037. <https://doi.org/10.1021/acsanm.1c00522>.
- (111) Nguyen, T.; Montemor, M. de F. Metal Oxide and Hydroxide–Based Aqueous Supercapacitors: From Charge Storage Mechanisms and Functional Electrode Engineering to Need-Tailored Devices. *Advanced Science* **2019**, *6* (9), 1801797. <https://doi.org/10.1002/advs.201801797>.
- (112) Deng, L.; Wang, J.; Zhu, G.; Kang, L.; Hao, Z.; Lei, Z.; Yang, Z.; Liu, Z.-H. RuO<sub>2</sub>/Graphene Hybrid Material for High Performance Electrochemical Capacitor. *Journal of Power Sources* **2014**, *248*, 407–415. <https://doi.org/10.1016/j.jpowsour.2013.09.081>.
- (113) Douard, C.; Athouël, L.; Brown, D.; Crosnier, O.; Rebmann, G.; Schilling, O.; Brousse, T. Electrode Design for MnO<sub>2</sub>-Based Aqueous Electrochemical Capacitors: Influence of Porosity and Mass Loading. *Materials* **2021**, *14* (11), 2990. <https://doi.org/10.3390/ma14112990>.
- (114) Lee, S.-M.; Park, Y.-J.; Lam, D. V.; Kim, J.-H.; Lee, K. Effects of Annealing on Electrochemical Performance in Graphene/V<sub>2</sub>O<sub>5</sub> Supercapacitor. *Applied Surface Science* **2020**, *512*, 145626. <https://doi.org/10.1016/j.apsusc.2020.145626>.
- (115) Sun, W.; Xiao, L.; Wu, X. Facile Synthesis of NiO Nanocubes for Photocatalysts and Supercapacitor Electrodes. *Journal of Alloys and Compounds* **2019**, *772*, 465–471. <https://doi.org/10.1016/j.jallcom.2018.09.185>.
- (116) Iqbal, M. Z.; Haider, S. S.; Zakar, S.; Alzaid, M.; Afzal, A. M.; Aftab, S. Cobalt-Oxide/Carbon Composites for Asymmetric Solid-State Supercapacitors. *Materials Research Bulletin* **2020**, *131*, 110974. <https://doi.org/10.1016/j.materresbull.2020.110974>.
- (117) Chen, S.; Zhu, J.; Wu, X.; Han, Q.; Wang, X. Graphene Oxide–MnO<sub>2</sub> Nanocomposites for Supercapacitors. *ACS Nano* **2010**, *4* (5), 2822–2830. <https://doi.org/10.1021/nn901311t>.
- (118) Choudhury, A.; Bonso, J. S.; Wunch, M.; Yang, K. S.; Ferraris, J. P.; Yang, D. J. In-Situ Synthesis of Vanadium Pentoxide Nanofibre/Exfoliated Graphene Nanohybrid and Its Supercapacitor Applications. *Journal of Power Sources* **2015**, *287*, 283–290. <https://doi.org/10.1016/j.jpowsour.2015.04.062>.
- (119) Kharade, P. M.; Thombare, J. V.; Babar, A. R.; Bulakhe, R. N.; Kulkarni, S. B.; Salunkhe, D. J. Electrodeposited Nanoflakes like Hydrophilic Co<sub>3</sub>O<sub>4</sub> as a Supercapacitor Electrode. *Journal of Physics and Chemistry of Solids* **2018**, *120*, 207–210. <https://doi.org/10.1016/j.jpcs.2018.04.035>.



- (120) Li, J.; Wang, Y.; Xu, W.; Wang, Y.; Zhang, B.; Luo, S.; Zhou, X.; Zhang, C.; Gu, X.; Hu, C. Porous Fe<sub>2</sub>O<sub>3</sub> Nanospheres Anchored on Activated Carbon Cloth for High-Performance Symmetric Supercapacitors. *Nano Energy* **2019**, *57*, 379–387. <https://doi.org/10.1016/j.nanoen.2018.12.061>.
- (121) Guan, Q.; Cheng, J.; Wang, B.; Ni, W.; Gu, G.; Li, X.; Huang, L.; Yang, G.; Nie, F. Needle-like Co<sub>3</sub>O<sub>4</sub> Anchored on the Graphene with Enhanced Electrochemical Performance for Aqueous Supercapacitors. *ACS Appl. Mater. Interfaces* **2014**, *6* (10), 7626–7632. <https://doi.org/10.1021/am5009369>.
- (122) Balducci, A.; Belanger, D.; Brousse, T.; Long, J. W.; Sugimoto, W. Perspective—A Guideline for Reporting Performance Metrics with Electrochemical Capacitors: From Electrode Materials to Full Devices. *J. Electrochem. Soc.* **2017**, *164* (7), A1487–A1488. <https://doi.org/10.1149/2.0851707jes>.
- (123) Zhang, S.; Pan, N. Supercapacitors Performance Evaluation. *Adv. Energy Mater.* **2015**, *5* (6), 1401401. <https://doi.org/10.1002/aenm.201401401>.
- (124) Gao, X.; Zhang, H.; Guo, E.; Yao, F.; Wang, Z.; Yue, H. Hybrid Two-Dimensional Nickel Oxide-Reduced Graphene Oxide Nanosheets for Supercapacitor Electrodes. *Microchemical Journal* **2021**, *164*, 105979. <https://doi.org/10.1016/j.microc.2021.105979>.
- (125) Shown, I.; Ganguly, A.; Chen, L.-C.; Chen, K.-H. Conducting Polymer-Based Flexible Supercapacitor. *Energy Science & Engineering* **2015**, *3* (1), 2–26. <https://doi.org/10.1002/ese3.50>.
- (126) Moosavifard, S. E.; Mohammadi, A.; Ebrahimnejad Darzi, M.; Kariman, A.; Abdi, M. M.; Karimi, G. A Facile Strategy to Synthesis Graphene-Wrapped Nanoporous Copper-Cobalt-Selenide Hollow Spheres as an Efficient Electrode for Hybrid Supercapacitors. *Chemical Engineering Journal* **2021**, *415*, 128662. <https://doi.org/10.1016/j.cej.2021.128662>.
- (127) Zhao, Y.; Shi, Z.; Li, H.; Wang, C.-A. Designing Pinecone-like and Hierarchical Manganese Cobalt Sulfides for Advanced Supercapacitor Electrodes. *J. Mater. Chem. A* **2018**, *6* (26), 12782–12793. <https://doi.org/10.1039/C8TA02438C>.
- (128) Geng, P.; Zheng, S.; Tang, H.; Zhu, R.; Zhang, L.; Cao, S.; Xue, H.; Pang, H. Transition Metal Sulfides Based on Graphene for Electrochemical Energy Storage. *Advanced Energy Materials* **2018**, *8* (15), 1703259. <https://doi.org/10.1002/aenm.201703259>.
- (129) Gao, Y.; Zhao, L. Review on Recent Advances in Nanostructured Transition-Metal-Sulfide-Based Electrode Materials for Cathode Materials of Asymmetric Supercapacitors. *Chemical Engineering Journal* **2022**, *430*, 132745. <https://doi.org/10.1016/j.cej.2021.132745>.
- (130) Venkateshalu, S.; Rangappa, D.; Grace, A. N. Hydrothermal Synthesis and Electrochemical Properties of CoS<sub>2</sub>-Reduced Graphene Oxide Nanocomposite for Supercapacitor Application. *Int. J. Nanosci.* **2018**, *17* (01n02), 1760020. <https://doi.org/10.1142/S0219581X17600201>.
- (131) Ma, T.; Chen, J.; Chen, M.; Liu, S.; Luo, J.; Zou, H.; Yang, W.; Chen, S. Nickel-Cobalt-Molybdenum Sulfides with Adjustable Morphology via Coprecipitation and Hydrothermal Conversion as High-Performance Electrodes for Asymmetric Supercapacitors. *Journal of Alloys and Compounds* **2020**, *838*, 155631. <https://doi.org/10.1016/j.jallcom.2020.155631>.
- (132) Du, N.; Zheng, W.; Li, X.; He, G.; Wang, L.; Shi, J. Nanosheet-Assembled NiS Hollow Structures with Double Shells and Controlled Shapes for High-Performance Supercapacitors. *Chemical Engineering Journal* **2017**, *323*, 415–424. <https://doi.org/10.1016/j.cej.2017.04.127>.
- (133) Cheng, S.; Shi, T.; Chen, C.; Zhong, Y.; Huang, Y.; Tao, X.; Li, J.; Liao, G.; Tang, Z. Construction of Porous CuCo<sub>2</sub>S<sub>4</sub> Nanorod Arrays via Anion Exchange for High-Performance Asymmetric Supercapacitor. *Sci Rep* **2017**, *7* (1), 6681. <https://doi.org/10.1038/s41598-017-07102-1>.
- (134) Dakshana, M.; Meyvel, S.; Malarvizhi, M.; Sathya, P.; Ramesh, R.; Prabhu, S.; Silambarasan, M. Facile Synthesis of CuCo<sub>2</sub>S<sub>4</sub> Nanoparticles as a Faradaic Electrode for High Performance Supercapacitor Applications. *Vacuum* **2020**, *174*, 109218. <https://doi.org/10.1016/j.vacuum.2020.109218>.

- (135) Yan, H.; Zhu, K.; Liu, X.; Wang, Y.; Wang, Y.; Zhang, D.; Lu, Y.; Peng, T.; Liu, Y.; Luo, Y. Ultra-Thin NiS Nanosheets as Advanced Electrode for High Energy Density Supercapacitors. *RSC Advances* **2020**, *10* (15), 8760–8765. <https://doi.org/10.1039/C9RA09486E>.
- (136) Yu, X. Y.; (David) Lou, X. W. Mixed Metal Sulfides for Electrochemical Energy Storage and Conversion. *Advanced Energy Materials* **2018**, *8* (3), 1701592. <https://doi.org/10.1002/aenm.201701592>.
- (137) Pei, L.; Yang, Y.; Chu, H.; Shen, J.; Ye, M. Self-Assembled Flower-like FeS<sub>2</sub>/Graphene Aerogel Composite with Enhanced Electrochemical Properties. *Ceramics International* **2016**, *42* (4), 5053–5061. <https://doi.org/10.1016/j.ceramint.2015.11.178>.
- (138) Patil, S. J.; Kim, J. H.; Lee, D. W. Graphene-Nanosheet Wrapped Cobalt Sulphide as a Binder Free Hybrid Electrode for Asymmetric Solid-State Supercapacitor. *Journal of Power Sources* **2017**, *342*, 652–665. <https://doi.org/10.1016/j.jpowsour.2016.12.096>.
- (139) Mohammadi, A.; Arsalani, N.; Tabrizi, A. G.; Moosavifard, S. E.; Naqshbandi, Z.; Ghadimi, L. S. Engineering RGO-CNT Wrapped Co<sub>3</sub>S<sub>4</sub> Nanocomposites for High-Performance Asymmetric Supercapacitors. *Chemical Engineering Journal* **2018**, *334*, 66–80. <https://doi.org/10.1016/j.cej.2017.10.029>.
- (140) Chen, Q.; Cai, D.; Zhan, H. Construction of Reduced Graphene Oxide Nanofibers and Cobalt Sulfide Nanocomposite for Pseudocapacitors with Enhanced Performance. *Journal of Alloys and Compounds* **2017**, *706*, 126–132. <https://doi.org/10.1016/j.jallcom.2017.02.189>.
- (141) Xu, L.; Lu, Y. One-Step Synthesis of a Cobalt Sulfide/Reduced Graphene Oxide Composite Used as an Electrode Material for Supercapacitors. *RSC Advances* **2015**, *5* (83), 67518–67523. <https://doi.org/10.1039/C5RA11711A>.
- (142) Lin, T.-W.; Dai, C.-S.; Tasi, T.-T.; Chou, S.-W.; Lin, J.-Y.; Shen, H.-H. High-Performance Asymmetric Supercapacitor Based on Co<sub>9</sub>S<sub>8</sub>/3D Graphene Composite and Graphene Hydrogel. *Chemical Engineering Journal* **2015**, *279*, 241–249. <https://doi.org/10.1016/j.cej.2015.05.011>.
- (143) Jia, Y.; Wan, H.; Chen, L.; Zhou, H.; Chen, J. Hierarchical Nanosheet-Based MoS<sub>2</sub>/Graphene Nanobelts with High Electrochemical Energy Storage Performance. *Journal of Power Sources* **2017**, *354*, 1–9. <https://doi.org/10.1016/j.jpowsour.2017.04.031>.
- (144) Zhou, R.; Han, C.; Wang, X. Hierarchical MoS<sub>2</sub>-Coated Three-Dimensional Graphene Network for Enhanced Supercapacitor Performances. *Journal of Power Sources* **2017**, *352*, 99–110. <https://doi.org/10.1016/j.jpowsour.2017.03.134>.
- (145) Jinlong, L.; Tongxiang, L.; Meng, Y.; Suzuki, K.; Miura, H. The Plume-like Ni<sub>3</sub>S<sub>2</sub> Supercapacitor Electrodes Formed on Nickel Foam by Catalysis of Thermal Reduced Graphene Oxide. *Journal of Electroanalytical Chemistry* **2017**, *786*, 8–13. <https://doi.org/10.1016/j.jelechem.2017.01.004>.
- (146) Bhat, T. S.; Patil, P. S.; Rakhi, R. B. Recent Trends in Electrolytes for Supercapacitors. *Journal of Energy Storage* **2022**, *50*, 104222. <https://doi.org/10.1016/j.est.2022.104222>.
- (147) Piwek, J.; Platek, A.; Fic, K.; Frackowiak, E. Carbon-Based Electrochemical Capacitors with Acetate Aqueous Electrolytes. *Electrochimica Acta* **2016**, *215*, 179–186. <https://doi.org/10.1016/j.electacta.2016.08.061>.
- (148) Demarconnay, L.; Raymundo-Piñero, E.; Béguin, F. A Symmetric Carbon/Carbon Supercapacitor Operating at 1.6 V by Using a Neutral Aqueous Solution. **2010**. <https://doi.org/10.1016/J.ELECOM.2010.06.036>.
- (149) Abbas, Q.; Ratajczak, P.; Babuchowska, P.; Comte, A. L.; Bélanger, D.; Brousse, T.; Béguin, F. Strategies to Improve the Performance of Carbon/Carbon Capacitors in Salt Aqueous Electrolytes. *J. Electrochem. Soc.* **2015**, *162* (5), A5148. <https://doi.org/10.1149/2.0241505jes>.
- (150) Ratajczak, P.; Jurewicz, K.; Skowron, P.; Abbas, Q.; Béguin, F. Effect of Accelerated Ageing on the Performance of High Voltage Carbon/Carbon Electrochemical Capacitors in Salt Aqueous Electrolyte. *Electrochimica Acta* **2014**, *130*, 344–350. <https://doi.org/10.1016/j.electacta.2014.02.140>.
- (151) Chae, J. H.; Chen, G. Z. 1.9V Aqueous Carbon–Carbon Supercapacitors with Unequal Electrode Capacitances. *Electrochimica Acta* **2012**, *86*, 248–254. <https://doi.org/10.1016/j.electacta.2012.07.033>.

- (152) Ruther, R. E.; Sun, C.-N.; Holliday, A.; Cheng, S.; Delnick, F. M.; Zawodzinski, T. A.; Nanda, J. Stable Electrolyte for High Voltage Electrochemical Double-Layer Capacitors. *J. Electrochem. Soc.* **2016**, *164* (2), A277. <https://doi.org/10.1149/2.0951702jes>.
- (153) Zhong, C.; Deng, Y.; Hu, W.; Qiao, J.; Zhang, L.; Zhang, J. A Review of Electrolyte Materials and Compositions for Electrochemical Supercapacitors. *Chemical Society Reviews* **2015**, *44* (21), 7484–7539. <https://doi.org/10.1039/C5CS00303B>.
- (154) Bujewska, P.; Gorska, B.; Fic, K. Redox Activity of Selenocyanate Anion in Electrochemical Capacitor Application. *Synthetic Metals* **2019**, *253*, 62–72. <https://doi.org/10.1016/j.synthmet.2019.04.024>.
- (155) Slesinski, A.; Matei-Ghimbeu, C.; Fic, K.; Béguin, F.; Frackowiak, E. Self-Buffered PH at Carbon Surfaces in Aqueous Supercapacitors. *Carbon* **2018**, *129*, 758–765. <https://doi.org/10.1016/j.carbon.2017.12.101>.
- (156) Galek, P.; Frackowiak, E.; Fic, K. Interfacial Aspects Induced by Saturated Aqueous Electrolytes in Electrochemical Capacitor Applications. *Electrochimica Acta* **2020**, *334*, 135572. <https://doi.org/10.1016/j.electacta.2019.135572>.
- (157) Tian, X.; Zhu, Q.; Xu, B. “Water-in-Salt” Electrolytes for Supercapacitors: A Review. *ChemSusChem* **2021**, *14* (12), 2501–2515. <https://doi.org/10.1002/cssc.202100230>.
- (158) Abdulagatov, I. M.; Zeinalova, A.; Azizov, N. D. Viscosity of Aqueous Na<sub>2</sub>SO<sub>4</sub> Solutions at Temperatures from 298 to 573K and at Pressures up to 40MPa. *Fluid Phase Equilibria* **2005**, *227* (1), 57–70. <https://doi.org/10.1016/j.fluid.2004.10.028>.
- (159) Cho, Y.-G.; Hwang, C.; Cheong, D. S.; Kim, Y.-S.; Song, H.-K. Gel/Solid Polymer Electrolytes Characterized by In Situ Gelation or Polymerization for Electrochemical Energy Systems. *Advanced Materials* **2019**, *31* (20), 1804909. <https://doi.org/10.1002/adma.201804909>.
- (160) Gajewski, P.; Béguin, F. Hydrogel–Polymer Electrolyte for Electrochemical Capacitors with High Volumetric Energy and Life Span. *ChemSusChem* **2020**, *13* (7), 1876–1881. <https://doi.org/10.1002/cssc.201903077>.
- (161) Yang, H.; Liu, Y.; Kong, L.; Kang, L.; Ran, F. Biopolymer-Based Carboxylated Chitosan Hydrogel Film Crosslinked by HCl as Gel Polymer Electrolyte for All-Solid-State Supercapacitors. *Journal of Power Sources* **2019**, *426*, 47–54. <https://doi.org/10.1016/j.jpowsour.2019.04.023>.
- (162) Rayung, M.; Aung, M. M.; Azhar, S. C.; Abdullah, L. C.; Su’ait, M. S.; Ahmad, A.; Jamil, S. N. A. M. Bio-Based Polymer Electrolytes for Electrochemical Devices: Insight into the Ionic Conductivity Performance. *Materials* **2020**, *13* (4), 838. <https://doi.org/10.3390/ma13040838>.
- (163) Karaman, B.; Çevik, E.; Bozkurt, A. Novel Flexible Li-Doped PEO/Copolymer Electrolytes for Supercapacitor Application. *Ionics* **2019**, *25* (4), 1773–1781. <https://doi.org/10.1007/s11581-019-02854-4>.
- (164) Çevik, E.; Bozkurt, A. Redox Active Polymer Metal Chelates for Use in Flexible Symmetrical Supercapacitors: Cobalt-Containing Poly(Acrylic Acid) Polymer Electrolytes. *Journal of Energy Chemistry* **2021**, *55*, 145–153. <https://doi.org/10.1016/j.jechem.2020.07.014>.
- (165) Alipoori, S.; Mazinani, S.; Aboutalebi, S. H.; Sharif, F. Review of PVA-Based Gel Polymer Electrolytes in Flexible Solid-State Supercapacitors: Opportunities and Challenges. *Journal of Energy Storage* **2020**, *27*, 101072. <https://doi.org/10.1016/j.est.2019.101072>.
- (166) Aswathy, N. R.; Palai, A. K.; Ramadoss, A.; Mohanty, S.; Nayak, S. K. Fabrication of Cellulose Acetate-Chitosan Based Flexible 3D Scaffold-like Porous Membrane for Supercapacitor Applications with PVA Gel Electrolyte. *Cellulose* **2020**, *27* (7), 3871–3887. <https://doi.org/10.1007/s10570-020-03030-y>.
- (167) Menzel, J.; Frackowiak, E.; Fic, K. Agar-Based Aqueous Electrolytes for Electrochemical Capacitors with Reduced Self-Discharge. *Electrochimica Acta* **2020**, *332*, 135435. <https://doi.org/10.1016/j.electacta.2019.135435>.
- (168) Aziz, S. B.; Brza, M. A.; Hamsan, H. M.; Kadir, M. F. Z.; Abdulwahid, R. T. Electrochemical Characteristics of Solid State Double-Layer Capacitor Constructed from Proton Conducting Chitosan-Based Polymer Blend Electrolytes. *Polym. Bull.* **2021**, *78* (6), 3149–3167. <https://doi.org/10.1007/s00289-020-03278-1>.

- (169) Wu, X.; Lian, M. Highly Flexible Solid-State Supercapacitor Based on Graphene/Polypyrrole Hydrogel. *Journal of Power Sources* **2017**, *362*, 184–191. <https://doi.org/10.1016/j.jpowsour.2017.07.042>.
- (170) Hu, X.; Fan, L.; Qin, G.; Shen, Z.; Chen, J.; Wang, M.; Yang, J.; Chen, Q. Flexible and Low Temperature Resistant Double Network Alkaline Gel Polymer Electrolyte with Dual-Role KOH for Supercapacitor. *Journal of Power Sources* **2019**, *414*, 201–209. <https://doi.org/10.1016/j.jpowsour.2019.01.006>.
- (171) Batisse, N.; Raymundo-Piñero, E. A Self-Standing Hydrogel Neutral Electrolyte for High Voltage and Safe Flexible Supercapacitors. *Journal of Power Sources* **2017**, *348*, 168–174. <https://doi.org/10.1016/j.jpowsour.2017.03.005>.
- (172) Yamagata, M.; Soeda, K.; Ikebe, S.; Yamazaki, S.; Ishikawa, M. Chitosan-Based Gel Electrolyte Containing an Ionic Liquid for High-Performance Nonaqueous Supercapacitors. *Electrochimica Acta* **2013**, *100*, 275–280. <https://doi.org/10.1016/j.electacta.2012.05.073>.
- (173) Amaral, M. M.; Venâncio, R.; Peterlevitz, A. C.; Zanin, H. Recent Advances on Quasi-Solid-State Electrolytes for Supercapacitors. *Journal of Energy Chemistry* **2022**, *67*, 697–717. <https://doi.org/10.1016/j.jechem.2021.11.010>.
- (174) Fei, H.; Yang, C.; Bao, H.; Wang, G. Flexible All-Solid-State Supercapacitors Based on Graphene/Carbon Black Nanoparticle Film Electrodes and Cross-Linked Poly(Vinyl Alcohol)–H<sub>2</sub>SO<sub>4</sub> Porous Gel Electrolytes. *Journal of Power Sources* **2014**, *266*, 488–495. <https://doi.org/10.1016/j.jpowsour.2014.05.059>.
- (175) Tran, T. N. T.; Chung, H.-J.; Ivey, D. G. A Study of Alkaline Gel Polymer Electrolytes for Rechargeable Zinc–Air Batteries. *Electrochimica Acta* **2019**, *327*, 135021. <https://doi.org/10.1016/j.electacta.2019.135021>.
- (176) Kim, D. K.; Kim, N. D.; Park, S.-K.; Seong, K.; Hwang, M.; You, N.-H.; Piao, Y. Nitrogen Doped Carbon Derived from Polyimide/Multiwall Carbon Nanotube Composites for High Performance Flexible All-Solid-State Supercapacitors. *Journal of Power Sources* **2018**, *380*, 55–63. <https://doi.org/10.1016/j.jpowsour.2018.01.069>.
- (177) Xu, Y.; Lin, Z.; Huang, X.; Liu, Y.; Huang, Y.; Duan, X. Flexible Solid-State Supercapacitors Based on Three-Dimensional Graphene Hydrogel Films. *ACS Nano* **2013**, *7* (5), 4042–4049. <https://doi.org/10.1021/nn4000836>.
- (178) Li, D.; Xu, Z.; Ji, X.; Liu, L.; Gai, G.; Yang, J.; Wang, J. Deep Insight into Ionic Transport in Polyampholyte Gel Electrolytes towards High Performance Solid Supercapacitors. *J. Mater. Chem. A* **2019**, *7* (27), 16414–16424. <https://doi.org/10.1039/C9TA01208G>.
- (179) Tao, F.; Qin, L.; Wang, Z.; Pan, Q. Self-Healable and Cold-Resistant Supercapacitor Based on a Multifunctional Hydrogel Electrolyte. *ACS Appl. Mater. Interfaces* **2017**, *9* (18), 15541–15548. <https://doi.org/10.1021/acsami.7b03223>.
- (180) Roy, B. K.; Tahmid, I.; Rashid, T. U. Chitosan-Based Materials for Supercapacitor Applications: A Review. *J. Mater. Chem. A* **2021**, *9* (33), 17592–17642. <https://doi.org/10.1039/D1TA02997E>.
- (181) Pal, B.; Matsoso, J. B.; Parameswaran, A. K.; Roy, P. K.; Lukas, D.; Luxa, J.; Marvan, P.; Azadmanjiri, J.; Hrdlicka, Z.; Jose, R.; Sofer, Z. Flexible, Ultralight, and High-Energy Density Electrochemical Capacitors Using Sustainable Materials. *Electrochimica Acta* **2022**, *415*, 140239. <https://doi.org/10.1016/j.electacta.2022.140239>.